IJSRM
INTERNATIONAL JOURNAL OF SCIENCE AND RESEARCH METHODOLOGY
An Official Publication of Human Journals

Human Journals
Research Article
January 2019 Vol.:11, Issue:3

Ab-Initio and Vibrational Studies on Free Base, Cationic and Derived from Antihistaminic Cyclizine Agent

IJSRM
INTERNATIONAL JOURNAL OF SCIENCE AND RESEARCH METHODOLOGY
An Official Publication of Human Journals

María J. Márquez, Maximiliano A. Iramain, Silvia Antonia Brandán*

Cátedra de Química General, Instituto de Química Inorgánica, Facultad de Bioquímica. Química y Farmacia, Universidad Nacional de Tucumán, Ayacucho 471, (4000) San Miguel de Tucumán, Tucumán, Argentina.

Submission: 25 December 2018
Accepted: 31 December 2018
Published: 30 January 2019

Keywords: Cyclizine, Structural Properties, Force Fields, Vibrational Analysis, DFT calculations.

ABSTRACT

Experimental available infrared, Attenuated Total Reflectance (ATR) and Raman spectra of cyclizine hydrochloride have been employed to perform the complete assignments of expected 120, 123 and 126 vibration modes for free base, cationic and hydrochloride species of antihistaminic cyclizine (CYC) agent combining the Scaled Quantum Mechanical Force Field (SQMFF) methodology with *Ab-initio* calculations. The harmonic force fields and the force constants are reported for first time for those three species of CYC by using the B3LYP/6-31G* method. The predicted infrared, Raman and ultraviolet-visible spectra show reasonable correlations with the corresponding experimental ones. The most low solvation energy value was observed for the free base of CYC, as compared with the corresponding to scopolamine, heroin, morphine, cocaine and tropane alkaloids. The geometrical parameters predicted for the three cyclizine species show that both phenyl rings are symmetric, as evidenced from the experimental structure. The N-CH_3 distances in the three species of CYC have showed that the free base in solution presents practically the same value than heroin and morphine in the same medium. This similarity in the values could be attributed to that in CYC the N-CH_3 group is linked only to a ring(piperazine), as in heroin and morphine and not to bicyclic rings as in cocaine, scopolamine and tropane alkaloids. The mapped Molecular Electrostatic Potentials (MEP) surfaces reveal different nucleophilic and/or electrophilic regions in the three species of CYC where probable reactions can take place. Natural bond orbital (NBO) studies show clearly that the high stabilities of free base and hydrochloride species are strongly related to the $\pi \rightarrow \pi^*$ transitions due to the two phenyl rings in their structures while atoms in molecules (AIM) analyses clearly supports the high stability of hydrochloride species in solution due to the two interactions, H24---H30 and ionic H43---Cl44 interaction, where the strong ionic interaction is visibly evidenced by their highest values of their topological properties.

1. INTRODUCTION

Our interest to study different species containing the >N-CH_3 group is due mainly to the wide range of biological properties that present the species with this group, such as tropane alkaloids, where these classes are known for the multiple effects they present ranging from the cure of pain to causing addiction [1-7]. Recent studies performed on the structural, electronic and topological properties for some alkaloids by using *Ab-Initio* calculations have shown that when the >N-CH_3 group is linked to fused or alone rings changes in the charges, in the electronic densities of rings, stabilization and solvation energies can be expected [7]. Besides, these calculations have revealed that the N-C distance between those two atoms belonging to group play a very important role in the stability of the species [7].On the other hand, the theoretical studies computed on the frontier orbitals of free base, cationic and hydrochloride species of anti-histaminic diphenhydramine agent, containing two >N-CH_3 groups, have suggested practically the same reactivities than that predicted for the cationic form of cocaine [3,7] while the vibrational studies of scopolamine, morphine, heroin, cocaine and tropane alkaloids and of diphenhydramine have demonstrated that in the solid phase and in aqueous solution the hydrochloride/hydrobromide form is clearly present as cationic one [1-3,5-8].For these reasons, the hydrochloride structures should be studied as free base, cationic and hydrochloride species [1-3,5-7]and, specifically in aqueous solution. Continuing with the studies of species that contain the >N-CH_3 group in its structure and, which are of great medicinal and pharmacological interest, in this opportunity the three forms of antihistaminic cyclizine agent were evaluated because cyclizine hydrochloride is a drug used to treatment of nausea, vomiting, and dizziness associated with motion sickness and, besides possesses anticholinergic, antihistaminic, central nervous system depressant, and local anesthetic effects [9-20]. The systematic name of cyclicine is 1-(diphenylmethyl)-4-methylpiperazine monohydrochloride while its IUPAC name is 1-benzhydryl-4-methylpiperazine hydrochloride. The experimental structure of cyclicine hydrochloride was determined by X-ray diffraction by Bertolasi *et al* [11] but, so far, the structural properties and vibrational assignments of those three species of cyclizine were not published. In this work, the theoretical structures of three cyclizine species were optimized by using the hybrid B3LYP/6-31G* level of theory in gas phase and in aqueous solution [21,22]. The studies in solution were performed with the integral equation formalism variant polarised continuum method (IEFPCM) because it scheme contemplates the solvent effects while the solvation energies were computed with the universal solvation model [23-25]. For those three cyclizine

species, atomic charges, molecular electrostatic potential, bond orders, frontier orbitals and topological properties were calculated together with the harmonic force fields by using the Scaled Quantum Mechanical Force Field (SQMFF) and transferable scaling factors [26-27].Then, the complete assignments for the three species were performed by using the corresponding force fields, internal normal coordinates and the experimental available infrared, Attenuated Total Reflectance (ATR) and Raman spectra of cyclizine hydrochloride [29-31]. In additional form and taking into account the wide range of biological activities that presents cyclizine, the reactivities and behaviours for its three species were predicted in both media by using the frontier orbitals [32,33] and global descriptors [34-42].

2. *Ab-Initio* calculations

The initial structure for cyclizine hydrochloride was that experimental determined by X-ray diffraction by Bertolasi *et al* [11]and taken from the available CIF file. The cationic and free base species were modelled respectively by using the *Gauss View* program [43]removing first the Cl atom from that initial structure of cyclizine hydrochloride and at continuation the H atom.The optimizations of three species in both media were carried out with the Revision A.02 of Gaussian program [44] and the hybrid B3LYP/6-31G* method [21,22] experimental available infrared, ATR and Raman spectra of cyclizine hydrochloride]. The three species were optimized in solution by using PCM and SMD calculations [23-25] while the volume changes that experiment these species in the two media were evaluated with the Moldraw program [45].The vibrational wavenumbers for the three species in both media were used to check the natures of the reached stationary points. Here, three types of atomic charges were studied which are Merz-Kollman (MK) [46], Mulliken and natural population (NPA) and, after that, the molecular electrostatic potentials and bond orders were also predicted for the three species in both media. Then, the NBO and AIM programs were employed to compute the main delocalization energies and topological properties [47-49]while the kinetics stabilities and reactivities of three species of cyclizine were investigated through the frontier orbitals and of a series of known descriptors [34-42]. In addition and, in order to perform the complete vibrational assignments for the three species of cyclizine, the normal internal coordinates and transferable scaling factors were used to compute the harmonic force fields with the SQMFF method and the Molvib program [26-28].Strong coupling between some vibrations modes were observed in the three species and, for these reasons, Potential Energy Distribution (PED) contributions ≥ 7% were in some cases considered during the vibrational

assignments of three species of cyclizine. On the other hand, the electronic spectra of all species were also predicted in water by using Time-dependent DFT calculations (TD-DFT) at the 6-31G* level of theory with the Gaussian 09 program [44].

3. RESULTS AND DISCUSSION

3.1. Dipole moment, volume and solvation energy

In **Table 1** it is possible to observe calculated total energies, dipole moments and volumes for the three species of cyclizine in gas and aqueous solution phases by using the B3LYP/6-31G* Method. In **Figure 1** can be seen the theoretical molecular structures of free base, cationic and hydrocloride species of cyclizine, atoms labelling and identification of their rings.Imaginary frequencies were obtained for the cationic species in aqueous solution and for the hydrochloride species in gas phase.

Table 1. Calculated total energies (*E*), dipole moments (μ) and volumes (V) of three species of cyclizine in gas and aqueous solution phases.

B3LYP/6-31G* Method				
Medium	E (Hartrees)	ZPVE	μ (D)	V (Å^3)
Free base				
GAS	-808.6494	-808.2828	0.13	309.3
PCM	-808.6602	-808.2918	0.17	313.2
Cationic				
GAS	-809.0385	-808.6566	13.94	312.4
PCM[#]	*-809.1304*	*-808.7475*	*18.10*	*311.5*
Hydrochloride				
GAS[#]	*-1269.4712*	*-1269.0918*	*8.24*	*334.6*
PCM	-1269.5060	-1269.1229	12.38	337.6

[#]Imaginary frequencies

The low solubility in water of cationic species could support that observation while a higher solubility for cyclizine hydrochloride justifies its existence in aqueous solution although the solubility for this species is strongly dependent of pH of solution, as was reported by Bohloko [14]. Thus, at pH=4 the solubility of cyclizine hydrochloride in pure water was found of 3.85mg/ml while when the pH increases at 6.8 the solubility decreases at 2.77mg/ml. The three species of cyclizine chemically can act as weak bases due to the presence of two N atoms in their structures [14]. Besides, the presence of Cl atom in the hydrochloride species increases the dipole moment value in solution because this species is probably hydrated with

water molecules, as justified by the volume expansion. Hence, the volume of this species increases in solution showing a volume variation of 3 $Å^3$.

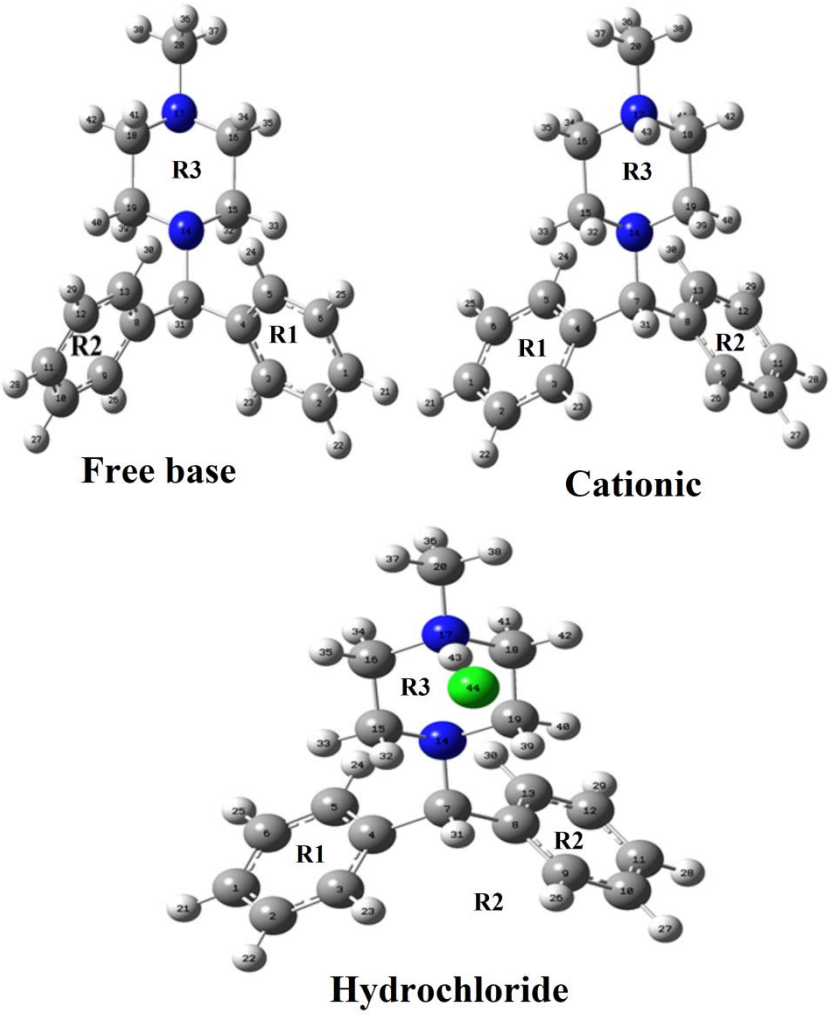

Figure 1. Theoretical molecular structures of free base, cationic and hydrochloride species of cyclizine, atoms labelling and identification of their rings.

Note that in the free base is also observed a strong volume expansion (3.9 $Å^3$), as compared with the hydrochloride species. In the same way, the cationic species in gas phase has a high dipole moment value. Here, we observed that when the energy values are corrected by Zero Point Vibrational Energy (ZPVE) in the three species the E values slightly decrease. In **Table 2** is compared the corrected (ΔG_c) and uncorrected solvation energy by the total non-electrostatic terms and by ZPVE for free base of cyclizine by using the B3LYP/6-31G* method with the reported values for the same species of other alkaloids [1,3,5-7]. For the free base of cyclizine, ΔG_c decreases from -34.25 kJ/mol up to -29.53 kJ/mol when both

corrections are applied. From Table 2 we observed that the free base of cyclizine presents the lower ΔG_c value than the other free base of alkaloids probably because in its structure there are two phenyl ring but no oxygen atom is observed, as in the other species where are observed between 3 and 4 O atoms [1,3,5-7].

Table 2. Corrected and uncorrected solvation energies by the total non-electrostatic terms and by ZPVE of free base of cyclizine by using the B3LYP/6-31G* method compared with the same species of other alkaloids.

B3LYP/6-31G* method[a]				
Solvation energy (kJ/mol)				
Reference	Condition	$\Delta G_{un}^{\#}$	ΔG_{ne}	ΔG_c
		Free base		
This Work	Cyclizine[a]	-23.60	5.93	-29.53
Reference 1	Morphine[b]	-47.74	13.17	-60.91
Reference 3	Cocaine[c]	-42.75	28.51	-71.26
Reference 6	Scopolamine[d]	-56.66	18.81	-75.47
Reference 5	Heroin[e]	-59.54	29.13	-88.67

$\Delta G_{un}^{\#}$= uncorrected solvation energy: defined as the difference between the total energies in aqueous solutions and the values in gas phase.

ΔG_{ne}= total non electrostatic terms: due to the cavitation, dispersion and repulsion energies.

ΔG_c= corrected solvation energies: defined as the difference between the uncorrected and non-electrostatic solvation energies.

3.2. Geometries in both media

Calculated geometrical parameters of three species of cyclizine in both media by using the 6-31G* level of theory are compared with the corresponding experimental ones [11] in **Table 3**by means of the Root-Mean-Square Deviation (RMSD) values. Very good correlations can be observed in the predicted parameters for the three species of cyclizine where the piperazine rings adopts clearly chair conformations and with values for bond lengths between 0.039 and 0.017 Å and for bond angles between 1.5 and 0.8º. The similarities in some parameters values show clearly that both phenyl rings are symmetric. In relation to the dihedral angles, the hydrochloride species in solution present the better results with a RMSD value of 4º while these values for free base and cationic species are very high around of177.2

and 174.2º,due to that the dihedral C7-N14-C15-C16, C7-N14-C19-C18, C20-N17-C16-C15 and C20-N17-C18-C19 angles change of signs in those two species, as detailed in Table 3.

Table 3. Comparison of calculated geometrical parameters of three species of cyclizine in both media with the corresponding experimental ones.

Parameters	B3LYP/6-31G* Method				Experimental [b]
	Free base		Cationic	Hydrochloride	
	Gas	PCM	Gas	PCM	
	Bond lengths (Å)				
N14-C7	1.474	1.483	1.474	1.486	1.480
N14-C15	1.468	1.475	1.469	1.473	1.462
N14-C19	1.468	1.475	1.469	1.473	1.463
N17-C16	1.459	1.466	1.459	1.501	1.489
N17-C18	1.459	1.466	1.459	1.501	1.489
N17-C20	1.453	1.459	1.453	1.489	1.490
C4-C7	1.530	1.530	1.531	1.530	1.524
C8-C7	1.530	1.530	1.531	1.530	1.524
C1-C2	1.392	1.395	1.394	1.395	1.379
C2-C3	1.394	1.397	1.396	1.397	1.383
C3-C4	1.396	1.401	1.398	1.401	1.384
C4-C5	1.399	1.403	1.402	1.403	1.392
C5-C6	1.392	1.395	1.394	1.395	1.379
C6-C1	1.395	1.398	1.397	1.397	1.375
C15-C16	1.525	1.524	1.527	1.520	1.511
C18-C19	1.525	1.524	1.527	1.520	1.511
N17-H43			1.000	1.062	0.913
H43-Cl44				2.040	2.089
RMSD[b]	**0.017**	**0.017**	**0.018**	**0.039**	
	Bond angles (º)				
C7-N14-C15	112.2	109.9	112.2	110.0	112.1
C7-N14-C19	112.2	109.9	112.2	110.0	112.1
C15-N14-C19	108.7	108.1	108.4	107.8	107.0
N14-C19-C18	110.7	111.7	110.5	111.7	109.8
N14-C15-C16	110.7	111.7	110.5	111.7	109.8
C15-C16-N17	110.9	111.3	110.8	111.0	110.9
C19-C18-N17	110.9	111.3	110.8	111.0	110.9
C16-N17-C18	110.2	108.2	110.0	110.1	110.1
C16-N17-C20	112.2	110.4	112.1	111.9	111.2
C18-N17-C20	112.2	110.4	112.1	111.9	111.3
C4-C7-C8	109.4	109.5	109.1	110.2	110.5
C4-C7-N14	112.0	112.9	111.9	112.4	110.6
C8-C7-N14	112.0	112.9	111.9	112.4	110.6
C3-C4-C5	118.5	118.3	118.5	118.4	118.4
C9-C8-C13	118.5	118.3	118.5	118.4	118.4
N-H-Cl				171.3	173.5
RMSD[b]	**0.9**	**1.5**	**0.8**	**1.3**	

Dihedral angles (º)					
C6-C5-C4-C7	177.8	177.3	177.4	178.0	178.6
C12-C13-C8-C7	-177.8	-177.3	-177.4	-178.0	-178.6
C4-C7-N14-C15	56.8	58.0	57.2	58.0	58.3
C4-C7-N14-C19	179.6	176.9	179.8	176.7	178.8
C7-N14-C15-C16	-176.7	176.0	-176.3	-179.9	-172.3
C7-N14-C19-C18	176.7	-176.0	176.3	179.9	172.3
C20-N17-C16-C15	-177.6	178.7	-177.6	178.2	176.7
C20-N17-C18-C19	177.6	-178.7	177.6	-178.2	-176.7
RMSD[b]	**177.2**	**174.2**	**177.2**	**4.0**	

[a]This work, [b]Ref [11]

For the hydrochloride species, the predicted N17-H43distance is of 2,040 Å, a value slightly low than the experimental one (2,089 Å) while the experimental N17---Cl44 distance is of 3.00 Å, notably lower than that predicted value of 3.095 Å. Here, interesting results are obtained when the separation N-C distances of >N-CH_3 groups belonging to the three cyclizine species and to different alkaloids are compared among them [1-7]. Thus, in **Table 4** are summarized the N-C distances of all species in gas and aqueous solution phases by using the B3LYP/6-31G* method. Then, in **Figure 2**can be easily seen their variations.

Table 4. Bond lengths observed between the N and C atoms of the N-CH_3 bonds belonging to the three cyclizine species in gas phase and in aqueous solution by using B3LYP/6-31G* calculations.

Species	N-CH_3 bond					
	Gas phase			Aqueous solution		
	Free base	Cationic	Hydrobromide	Free base	Cationic	Hydrobromide
Cyclizine	1.453	1.453	#	1.459	#	1.489
Scopolamine	1.462	1.492	1.491	1.466	1.491	1.493
Heroin	1.453	1.501	1.483	1.460	1.498	1.492
Morphine	1.453	1.500	1.483	1.460	1.497	1.493
Cocaine	1.459	1.493	1.487	1.467	1.492	1.494
Tropane	1.458	1.496	1.478	1.467	1.491	1.486

[#]Imaginary frequencies

In gas phase, the lowest values are observed in free base and cationic species of cyclizine while the cationic species of all alkaloids present the higher distances, in particular, heroin and morphine. These higher N-C distances observed in heroin and morphine could be justified by the absence of pyrrolidine rings in their structures, permitting this way, the higher

elongations of these bonds. In these species, obviously, the presence of positive charges on N atoms of N-CH_3groups increase the N-C distances, as compared with the free bases. Note that the free bases of all species present the lower distances because these species are not charged. In aqueous solution, the hydrochloride species of cyclizine increases the N-C distance presenting the lower value the species corresponding to tropane. The free bases of all species in solution increase their values and, in particular, the hydrochloride species of tropane alkaloid has the lower distance. The low values observed in the tropane could be associated to that the N-CH_3group is linked to fused piperidine and pyrrolidine rings diminishing the N-C distances. Moreover, the free base of cyclizine in solution has practically the same value than the species corresponding to heroin and morphine in the same medium. This similarity in the values could be attributed to that N-CH_3 group in cyclizine is linked only to a piperazine ring, as in heroin and morphine and not to bicyclic rings as in cocaine, scopolamine and tropane alkaloids. Evidently, the N-C distances are shortened when the N-CH_3 group is linked to two fused rings.

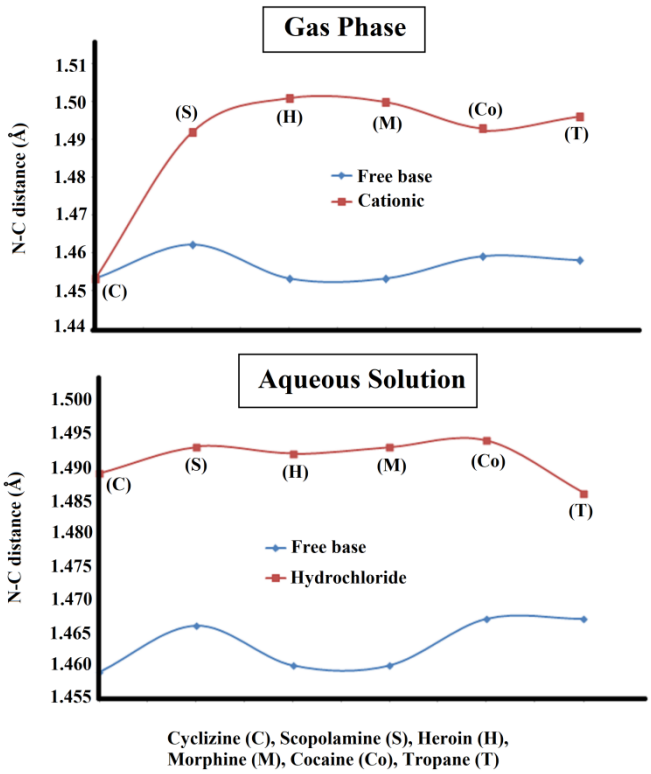

Figure 2. Calculated N-C distances corresponding to N-CH_3 groups of free base, cationic and hydrochloride species of cyclizine compared with the corresponding to other alkaloids in both media by using the B3LYP/6-31G* method.

3.3. Charges, molecular electrostatic potential and bond orders studies

The charges studies for the three species of cyclizine are very useful because the presences of two symmetric phenyl rings and of a piperazine ring in their structures confer to these species interesting properties. Here, only some Mulliken, Merz-Kollman (MK) and NPA charges on C and N atoms were studied for those three species in both media by using the 6-31G* level of theory. In **Table 5**are presented those three charges for the three species of cyclicine in gas phase and in aqueous solution by using B3LYP/6-31G* calculations together with the Molecular Electrostatic Potentials (MEP) and bond orders, expressed as Wiberg indexes.

Table 5. Mulliken, Merz-Kollman and NPA charges (a.u.), MEP (a.u.) and bond orders, expressed as Wiberg indexes for the three species of cyclicine in gas phase and in aqueous solution by using B3LYP/6-31G* calculations.

Free base										
	GAS					PCM				
Atoms	MK	Mulliken	NPA	MEP	BO	MK	Mulliken	NPA	MEP	BO
4 C	0.315	0.141	-0.038	-14.737	4.004	0.536	0.143	-0.039	-14.736	4.004
7 C	-0.620	-0.077	-0.065	-14.702	3.934	-1.488	-0.094	-0.068	-14.703	3.937
8 C	0.315	0.141	-0.038	-14.737	4.004	0.535	0.143	-0.039	-14.736	4.004
14 N	-0.114	-0.431	-0.516	-18.358	3.113	0.063	-0.423	-0.507	-18.358	3.106
15 C	-0.110	-0.128	-0.268	-14.725	3.862	-0.130	-0.128	-0.273	-14.725	3.865
16 C	-0.116	-0.120	-0.265	-14.723	3.874	-0.052	-0.127	-0.269	-14.723	3.874
17 N	-0.217	-0.382	-0.507	-18.363	3.118	-0.267	-0.381	-0.503	-18.363	3.109
18 C	-0.116	-0.120	-0.265	-14.723	3.874	-0.052	-0.127	-0.269	-14.723	3.874
19 C	-0.110	-0.128	-0.268	-14.725	3.862	-0.131	-0.128	-0.273	-14.725	3.865
20 C	-0.315	-0.289	-0.467	-14.725	3.818	-0.315	-0.291	-0.470	-14.726	3.819
	Cationic GAS					Hydrochloride PCM				
Atoms	MK	Mulliken	NPA	MEP	BO	MK	Mulliken	NPA	MEP	BO
4 C	0.388	0.129	-0.068	-14.639	4.002	0.463	0.136	-0.048	-14.721	4.004
7 C	-0.916	-0.095	-0.065	-14.587	3.917	-1.214	-0.102	-0.070	-14.683	3.928
8 C	0.388	0.129	-0.068	-14.639	4.002	0.463	0.136	-0.048	-14.721	4.004
14 N	-0.199	-0.421	-0.513	-18.215	3.120	-0.166	-0.430	-0.513	-18.328	3.094
15 C	0.094	-0.151	-0.291	-14.564	3.846	0.082	-0.156	-0.294	-14.688	3.846
16 C	-0.240	-0.175	-0.262	-14.526	3.782	-0.259	-0.157	-0.266	-14.660	3.816
17 N	0.025	-0.491	-0.452	-18.056	3.468	0.315	-0.478	-0.479	-18.228	3.388
18 C	-0.240	-0.175	-0.262	-14.526	3.782	-0.259	-0.157	-0.266	-14.660	3.816
19 C	0.094	-0.151	-0.291	-14.564	3.846	0.082	-0.156	-0.294	-14.688	3.846
20 C	-0.420	-0.334	-0.475	-14.522	3.711	-0.463	-0.312	-0.472	-14.664	3.744

The modifications in the three charges for all cyclizine species in both media can be clearly observed in **Figure 3**.

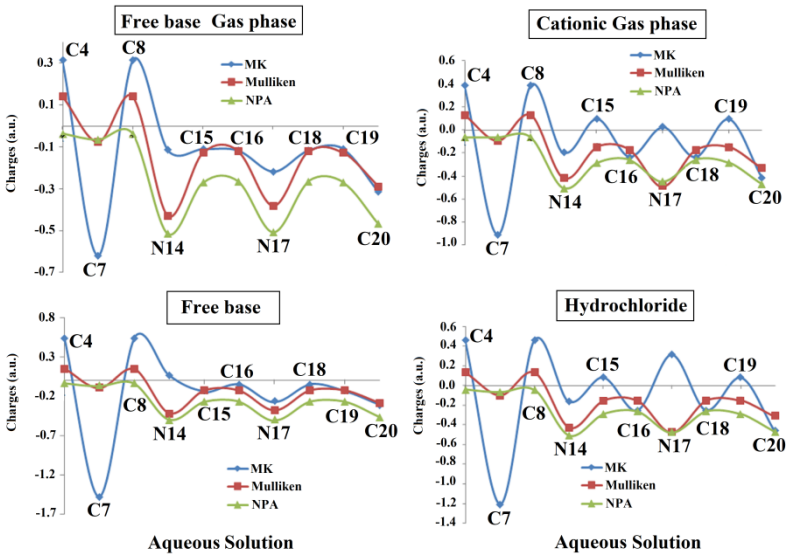

Figure 3. Calculated MK, Mulliken and NPA charges on free base, cationic and hydrochloride species of cyclizine in both media by using the B3LYP/6-31G* method.

The deep analyses of those charges show that: (i) the values of three charges are different among them and, where the MK charges show higher variations, (ii) the most negative MK values are observed on the C7 atoms of three species and the most positive values on the C4 and C8 atoms, (iii) the most negative Mulliken and NPA charges are observed on the N14 and N17 atoms and the most positive values on the C4 and C8 atoms, (iv) in solution, the Mulliken and NPA charges on all atoms of free base tend to approach each other, (v) the MK charges on the C15, N17 and C19 atoms change if signs in the cationic and hydrochloride species, showing this latter species in solution the higher value (0.315 a.u.). The most important results observed from Table 5 are the similarity among the properties for the C4 and C8 atoms, which indicate that both phenyl rings are equivalents.

The MEP values observed from Table 5 do not show significant difference among them, but when the mapped surfaces are graphed in **Figure 4** we can easily see the notable differences among the three surfaces. Hence, the MEP surface of free base in gas phase show strong red colours on the N17 atom due to its lone pairs indicating a clear nucleophilic site on that atom while soft yellow and blue colours are observed on the phenyl rings and H atoms of these rings, respectively. On the remaining atoms of piperazine ring the surfaces show green colours indicative of inert places.

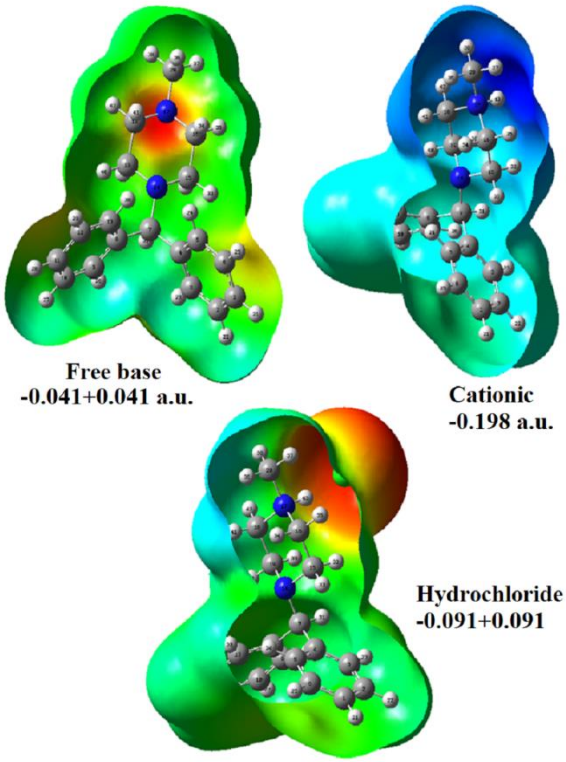

Figure 4. Calculated electrostatic potential surfaces on the molecular surfaces of the free base, cationic and hydrochloride species of cyclizine. Color ranges are indicated in units a.u. B3LYP functional and 6-31G* basis set. Isodensity value of 0.005.

The cationic species of cyclizine in gas phase shows two regions with different tonalities of blue color, showing the darkest regions on the atoms of the piperazine ring, as expected because it species is positively charged and, for this reason, present only electrophilic sites. The MEP surface of hydrochloride species in solution presents a strong red colour around the Cl atom which indicates nucleophilic sites while light blue colours are observed on H atoms of CH_2 and C-H groups of piperazine and phenyl rings, respectively. This study evidently reveals the different regions expected in the three species of cyclizine where probable reactions with nucleophilic and/or electrophilic reactive take place.

The Bond Orders (BO), expressed as Wiberg indexes, were also studied for the three species of cyclizine in both media by using the 6-31G* level of theory. The values are summarized in Table 5. When these values are exhaustively analysed for the three species in the two media it is possible to see the lower values for the N14 and N17 atoms while the C4 and C8 atoms present the same values in both media, confirming that both phenyl rings are symmetric in the three species. On the other side, practically the same values for the free base in both

media are observed. When now the values for the cationic and hydrochloride species in gas phase and in solution, respectively are evaluated the BO for the N17 atoms increase the values in both species (3.468 in the cationic and 3.388 in the hydrochloride), as compared with the lower value for free basein solution (3.109). In general, only differences in the BO from C15 atoms up to C20 atoms are observed for the three species.

3.4. NBO and AIM studies

The main donor-acceptor energy interactions are useful properties to explore the stabilities of three cyclizine species in both media computing the second order perturbation theory analysis of Fock matrix in NBO Basis with the NBO program [47]. Here, the main delocalization energies for these species in both media by using the B3LYP/6-31G* method are descript in **Table 6**. Note that for both free base and cationic species only are observed $\Delta E_{\pi\rightarrow\pi^*}$interactions which are related to the C=C bonds of phenyl rings while in the hydrochloride species are predicted other two different $\Delta E_{\sigma\rightarrow LP^*}$and $\Delta E_{LP\rightarrow LP^*}$interactions attributed to N17, H43 and Cl44atoms.Obviously, these three interactions confer to the hydrochloride species a high stability in solution with an ΔE_{TOTAL} value of 2970.56 kJ/mol. The low value obtained for the cationic species in gas phase could be justified because this species only can exist in solution.

Table 6. Main delocalization energies (in kJ/mol) for the three species of cyclicine in gas and aqueous solution phases by using B3LYP/6-31G* calculations.

B3LYP/6-31G*[a]			
Delocalization	Free base		Cationic
	Gas	PCM	Gas
$\pi C1\text{-}C2\rightarrow\pi^*C3\text{-}C4$	81.93	82.05	44.56
$\pi C1\text{-}C2\rightarrow\pi^*C5\text{-}C6$	84.48	84.48	43.68
$\pi C3\text{-}C4\rightarrow\pi^*C1\text{-}C2$	87.49	87.40	40.00
$\pi C3\text{-}C4\rightarrow\pi^*C5\text{-}C6$	79.96	80.30	39.92
$\pi C5\text{-}C6\rightarrow\pi^*C1\text{-}C2$	83.43	83.39	39.71
$\pi C5\text{-}C6\rightarrow\pi^*C3\text{-}C4$	85.65	85.69	43.05
$\pi C8\text{-}C9\rightarrow\pi^*C10\text{-}C11$	87.49	87.40	40.00
$\pi C8\text{-}C9\rightarrow\pi^*C12\text{-}C13$	79.96	80.34	39.92
$\pi C10\text{-}C11\rightarrow\pi^*C8\text{-}C9$	81.93	82.09	44.56
$\pi C10\text{-}C11\rightarrow\pi^*C12\text{-}C13$	84.48	84.48	43.68
$\pi C12\text{-}C13\rightarrow\pi^*C8\text{-}C9$	85.65	85.69	43.05

$\pi C12\text{-}C13 \rightarrow \pi^*C10\text{-}C11$	83.43	83.39	39.71
	1005.88	**1006.7**	**501.84**

Delocalization	Hydrochloride
	PCM
$\pi C1\text{-}C6 \rightarrow \pi^*C2\text{-}C3$	85.98
$\pi C1\text{-}C6 \rightarrow \pi^*C4\text{-}C5$	85.31
$\pi C2\text{-}C3 \rightarrow \pi^*C1\text{-}C6$	84.56
$\pi C2\text{-}C3 \rightarrow \pi^*C4\text{-}C5$	88.66
$\pi C4\text{-}C5 \rightarrow \pi^*C1\text{-}C6$	87.40
$\pi C4\text{-}C5 \rightarrow \pi^*C2\text{-}C3$	83.01
$\pi C8\text{-}C9 \rightarrow \pi^*C10\text{-}C11$	85.02
$\pi C8\text{-}C9 \rightarrow \pi^*C12\text{-}C13$	81.09
$\pi C10\text{-}C11 \rightarrow \pi^*C8\text{-}C9$	84.10
$\pi C10\text{-}C11 \rightarrow \pi^*C12\text{-}C13$	85.60
$\pi C12\text{-}C13 \rightarrow \pi^*C8\text{-}C9$	85.15
$\pi C12\text{-}C13 \rightarrow \pi^*C10\text{-}C11$	82.09
$\Delta E_{\pi \rightarrow \pi^*}$	**1017.97**
$\sigma C16\text{-}N17 \rightarrow LP^*(1)H43$	55.47
$\sigma N17\text{-}C18 \rightarrow LP^*(1)H43$	55.47
$\sigma N17\text{-}C20 \rightarrow LP^*(1)H43$	62.32
$\Delta E_{\sigma \rightarrow LP^*}$	**173.26**
$LP(1)N17 \rightarrow LP^*(1)H43$	1483.35
$LP(4)Cl44 \rightarrow LP^*(1)H43$	295.98
$\Delta E_{LP \rightarrow LP^*}$	**1779.33**
ΔE_{TOTAL}	**2970.56**

[a]This work

These studies show clearly that the high stabilities of free base and hydrochloride species are strongly related to the presence of two phenyl ring in their structures.

NBO studies have demonstrated the high stability of hydrochloride species of cyclizine in aqueous solution and the particular polynomial relation found between the total energies for these species in solution and their molecular weights. The Bader's theory is also very interesting to investigate the stabilities of different species due to the presence of inter or intra-molecular interactions knowing their topological properties [48,49]. Accordingly, in the Bond Critical Points (BCPs) and Ring Critical Points (RCPs) the electron density, $\rho(r)$, the Laplacian values, $\nabla^2\rho(r)$, the eigenvalues $(\lambda 1, \lambda 2, \lambda 3)$ of the Hessian matrix and, the $|\lambda 1|/\lambda 3$ ratio were computed for the three cyclizine species. In **Table 7** are presented the results of

those mentioned parameters by using the B3LYP/6-31G* method. First, it is necessary to clarify that the interaction is ionic or highly polar covalent when $\lambda 1/\lambda 3 < 1$ and $\nabla^2\rho(r) > 0$ (closed-shellinter action).

Table 7. Analysis of the Bond Critical Points (BCPs) and Ring critical point (RCPs) for the three species of cyclicinein gas and aqueous solution phases by using the B3LYP/6-31G* method.

B3LYP/6-31G* Method					
Free base					
Gas phase					
Parameter#	H24---H30	RCPN	RCP1	RCP2	RCP3
ρ(r)	0.0050	0.0050	0.0201	0.0201	0.0190
$\nabla^2\rho(r)$	0.0194	0.0196	0.1617	0.1617	0.1309
λ1	-0.0030	-0.0023	-0.0151	-0.0151	-0.0131
λ2	-0.0008	0.0009	0.0852	0.0852	0.0568
λ3	0.0233	0.0211	0.0915	0.0915	0.0872
|λ1|/λ3	0.1288	0.1090	0.1650	0.1650	0.1502
Distances (Å)	2.448				
Aqueous solution					
Parameter#	H24---H30	RCPN	RCP1	RCP2	RCP3
ρ(r)	0.0057	0.0055	0.0200	0.0200	0.0191
$\nabla^2\rho(r)$	0.0222	0.0219	0.1607	0.1607	0.1292
λ1	-0.0046	-0.0029	-0.0149	-0.0149	-0.0138
λ2	-0.0022	0.0020	0.0843	0.0843	0.0536
λ3	0.0291	0.0227	0.0913	0.0913	0.0894
|λ1|/λ3	0.1581	0.1278	0.1632	0.1632	0.1544
Distances (Å)	2.363				
Cationic					
Gas phase					
Parameter#	H24---H30	RCPN	RCP1	RCP2	RCP3
ρ(r)	0.0058	0.0054	0.0201	0.0201	0.0186
$\nabla^2\rho(r)$	0.0224	0.0219	0.1616	0.1616	0.1228
λ1	-0.0047	-0.0025	-0.0151	-0.0151	-0.0126
λ2	-0.0026	0.0027	0.0855	0.0855	0.0563

λ3	0.0298	0.0216	0.0912	0.0912	0.0792	
|λ1|/λ3	0.1577	0.1157	0.1656	0.1656	0.1591	
Distances (Å)	2.355					
Hydrochloride						
Aqueous solution						
Parameter[#]	H24---H30	RCPN	RCP1	RCP2	RCP3	H43---Cl44
ρ(r)	0.0061	0.0056	0.0200	0.0200	0.0186	0.0408
$\nabla^2\rho(r)$	0.0236	0.0228	0.1608	0.1608	0.1227	0.0757
λ1	-0.0051	-0.0029	-0.0149	-0.0149	-0.0135	-0.0519
λ2	-0.0028	0.0027	0.0843	0.0843	0.0531	-0.0518
λ3	0.0316	0.0229	0.0913	0.0913	0.0832	0.1795
|λ1|/λ3	0.1614	0.1266	0.1632	0.1632	0.1623	0.2891
Distances (Å)	2.329					

Thus, in the three species of cyclizine are observed H24---H30 interactions but, in particular, the hydrochloride species in solution has also the ionic H43---Cl44 interaction. The RCPN is the new RCP formed due to the H24---H30 interactions while RCP1 and RCP2 are RCP corresponding to the phenyl R1 and R2 rings and, RCP3 correspond to piperazine ring. Note that the topological properties of H24---H30 interactions present higher values in the hydrochloride species probably because the distance is shortest in this species. Other very important result is that the characteristic of RCP1 are exactly similar to RCP2, confirming that both rings are symmetric. This study clearly supports the high stability of hydrochloride species in solution due to the two interactions, H24---H30 and ionic H43---Cl44 interaction. Obviously, the ionic interaction is stronger than the other one due to the high electronegativity of Cl atom, as revealed by the highest values of their topological properties. The molecular graphic for the hydrochloride species with the details of their BCP and RCP can be seen in **Figure 5**.

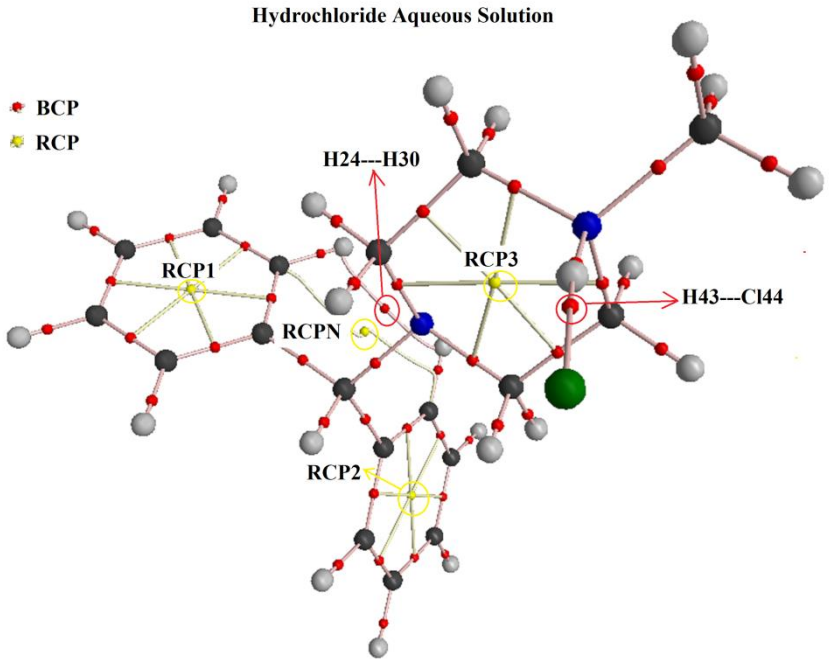

Figure 5. Molecular graphic for the hydrochloride species of cyclizine in solution showing the geometry of all their BCPs and RCPs by using the B3LYP/6-31G* method.

3.5. Frontier orbitals and global descriptors studies

Previous studies on some alkaloids have evidenced that the presence of N-CH_3 groups linked to two fused piperidine and pyrrolidine rings, such as in scopolamine, cocaine and tropane alkaloids produces changes in some of their properties including in their reactivities [1-7], where tropane is the less reactive species while cocaine present the higher reactivity, as compared with scopolamine, cocaine, heroin, morphine and tropane. Hence, the frontier orbitals [32,33] for the free base, cationic and hydrochloride species of cyclizine species and some descriptors [34-42]were also calculated by using the hybrid B3LYP/6-31G* level of theory and compared with the values reported for those mentioned alkaloids [1-7]. Thus, the HOMO, LUMO and energy band gap can be seen in **Table 8** while the chemical potential (μ), electronegativity (χ), global hardness (η), global softness (S), global electrophilicity index (ω) and global nucleophilicity index ((E) descriptors [34-42]are presented in **Table 9**.

Table 8. Frontier molecular HOMO and LUMO orbitals and gap values for the three cyclizine species compared with alkaloid species in gas and aqueous solution phases by using the B3LYP/6-31G* level of theory.

Free base/Gas phase						
Orbital	Scopolamine[#.b]	Heroin[b]	Morphine[b]	Cocaine[b]	Tropane[b]	cyclizine[a]
HOMO	-5.765	-5.749	-5.567	-5.9267	-5.4945	-5.7057
LUMO	-0.3646	-0.0927	0.0374	-1.0687	2.0561	-0.3111
|GAP|	5.4004	5.6563	5.6044	4.8580	7.5506	5.3946
Free base /Aqueous solution						
Orbital	Scopolamine[#.b]	Heroin[b]	Morphine[b]	Cocaine[b]	Tropane[b]	cyclizine[a]
HOMO	-5.8338	-5.7471	-5.3367	-6.0125	-5.6725	-5.8388
LUMO	-0.358	-0.1057	0.1383	-1.0638	1.9886	-0.3321
|GAP|	5.4758	5.6414	5.475	4.9487	7.6611	5.5067
Cationic/Gas phase						
Orbital	Scopolamine[#.b]	Heroin[b]	Morphine[b]	Cocaine[b]	Tropane[b]	cyclizine[a]
HOMO	-8.8482	-8.7639	-8.5413	-9.3162	-12.9365	-8.8187
LUMO	-3.2126	-3.3371	-3.3524	-3.8694	-3.377	-3.2364
|GAP|	5.6356	5.4268	5.1889	5.4468	9.5595	5.5823
Hydrochloride/Aqueous solution						
Orbital	Scopolamine[#.b]	Heroin[b]	Morphine[b]	Cocaine[b]	Tropane[b]	cyclizine[a]
HOMO	-5.0022	-5.1808	-5.1973	-4.9833	-4.9043	-4.9421
LUMO	0.4004	-0.7339	-0.6133	-1.302	1.0076	-0.7262
|GAP|	5.4026	4.4469	4.584	3.6813	5.9119	4.2159

[#]Hydrobromide, [a]This work, [b]From Ref [7]

Obviously, the optimized cationic and hydrochloride species in solution and in gas phase respectively were not considered in this study due to their imaginary frequencies.

Table 9. Chemical potential (μ), electronegativity (χ), global hardness (η), global softness (S) and global electrophilicity(ω) and nucleophilicity (E) indexes descriptors for hydrochloride cyclizine and alkaloid species in gas and aqueous solution phases by using the B3LYP/6-31G* level of theory.

Free base/Gas phase[a]						
Descriptor	Scopolamine[#.b]	Heroin[b]	Morphine[b]	Cocaine[b]	Tropane[b]	cyclizine[a]
χ	-2.462	-2.6512	-2.7209	-2.2541	-3.4123	-2.6973
μ	-2.9289	-3.2329	-3.1709	-3.4397	-2.1787	-3.0084
η	2.462	2.6512	2.7209	2.2541	3.4123	2.6973
S	0.2031	0.1886	0.1838	0.2218	0.1465	0.1854
ω	1.7421	1.9711	1.8476	2.6244	0.6955	1.6777
E	-7.2107	-8.5711	-8.6274	-7.7534	-7.4343	-8.1146
Free base /Aqueous solution[a]						
Descriptor	Scopolamine[#.b]	Heroin[b]	Morphine[b]	Cocaine[b]	Tropane[b]	cyclizine[a]
χ	-2.7013	-2.2235	-2.292	-1.8407	-2.956	-2.7534
μ	-2.3009	-2.9574	-2.9053	-3.1427	-1.9483	-3.0855
η	2.7013	2.2235	2.292	1.8407	2.956	2.7534
S	0.1851	0.2249	0.2182	0.2716	0.1691	0.1816
ω	0.9799	1.9667	1.8414	2.6828	0.6421	1.7288
E	-6.2154	-6.5755	-6.6589	-5.7845	-5.7592	-8.4953
Cationic/Gas phase[a]						
Descriptor	Scopolamine[#.b]	Heroin[b]	Morphine[b]	Cocaine[b]	Tropane[b]	cyclizine[a]
χ	-2.8178	-2.7134	-2.5945	-2.7234	-4.7798	-2.7912
μ	-6.0304	-6.0505	-5.9469	-6.5928	-8.1567	-6.0276
η	2.8178	2.7134	2.5945	2.7234	4.7798	2.7912
S	0.1774	0.1843	0.1927	0.1836	0.1046	0.1791
ω	6.4529	6.7459	6.8155	7.9799	6.9598	6.5083
E	-16.9925	-16.4174	-15.4288	-17.9548	-38.9872	-16.8238
Hydrochloride/Aqueous solution[a]						
Descriptor	Scopolamine[#.b]	Heroin[b]	Morphine[b]	Cocaine[b]	Tropane[b]	cyclizine[a]
χ	-2.7013	-2.2235	-2.292	-1.8407	-2.956	-2.1080
μ	-2.3009	-2.9574	-2.9053	-3.1427	-1.9483	-2.8342
η	2.7013	2.2235	2.292	1.8407	2.956	2.1080
S	0.1851	0.2249	0.2182	0.2716	0.1691	0.2372
ω	0.9799	1.9667	1.8414	2.6828	0.6421	1.9053
E	-6.2154	-6.5755	-6.6589	-5.7845	-5.7592	-5.9742

[#]Hydrobromide, [a]This work, [b]From Ref [7]

$\chi = -[E(LUMO) - E(HOMO)]/2$; $\mu = [E(LUMO) + E(HOMO)]/2$; $\eta = [E(LUMO) - E(HOMO)]/2$;

$S = \frac{1}{2}\eta$; $\omega = \mu^2/2\eta$; $E = \mu * \eta$

Figure 6 shows clearly the differences among the cyclizine species in the two studied media with the alkaloids values.

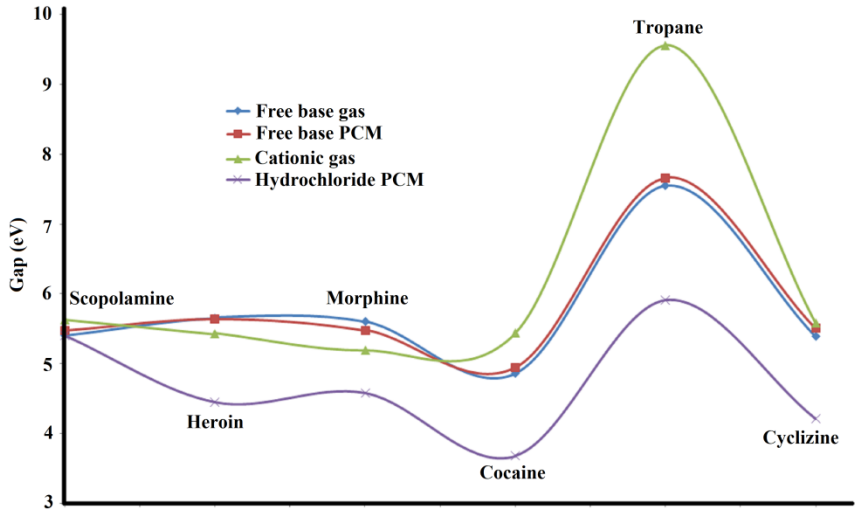

Figure 6. Calculated gap values of free base, cationic and hydrochloride species of cyclizine compared with the corresponding to other alkaloids in both media by using the B3LYP/6-31G* method.

Note first the proximities in the gap values for all species of scopolamine while the free bases of all species have the same behaviours in both media (lines red and blue colours). The tropane species are evidently the less reactive while the hydrochloride species of cocaine is the most reactive in solution together with the cyclizine species. Here, the hydrochloride/hydrobromide species evidence clearly the higher reactivities in solution and, for these reasons; the hydrochloride or hydrobromide species are highly used as a drug in pharmacology due to their quick assimilations. Analyzing the electrophilicity and nucleophilicity indexes because they show the higher changes, from Table 9 we observed that the free base of cocaine in gas phase presents the higher value while the same species of morphine the most negative E index. In solution, the free base of cocaine shows the higher ω index while the cyclizine species has the higher E index. The cationic species of cocaine in

gas phase has the higher ω index while the tropane species the highest E index (-38.9872 eV). Probably, the low reactivity of tropane is associated to its high E index value as a consequence of their two fused piperidine and pyrrolidine rings and, also to the absence of other atoms or groups in its structure. In relation to the hydrochloride species in solution, the cocaine species has the higher ω index while the morphine species the highest E index (-6.6589 eV).

3.6. Vibrational analyses

The three cyclizine species in both media were optimized with C_1symmetries by using the hybrid B3LYP/6-31G* method. The numbers of vibration normal modes expected for the free base, cationic and hydrochloride speciesare 120, 123 and 126 respectively and, all vibration modes present activities in the infrared and Raman spectra. In this analysis, the experimental infrared, ATR and Raman spectra for the hydrochloride species of cyclizine were taken from those available in the literature [29-31]. Both spectra were compared with the corresponding predicted by calculations for those three species in **Figures 7** and **8**. The predicted IR and Raman spectra for the three species show reasonable concordance with the corresponding experimental ones.

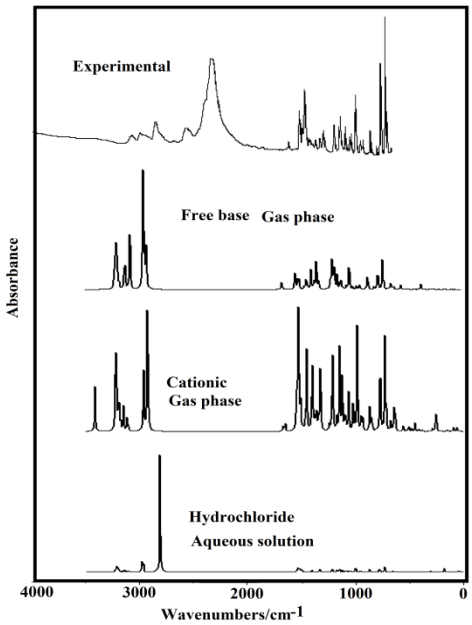

Figure 7. Experimental infrared spectrum of hydrochloride cyclizine species[29] compared with the corresponding predicted for the free base, cationic and hydrochloride species by using B3LYP/6-31G* level of theory.

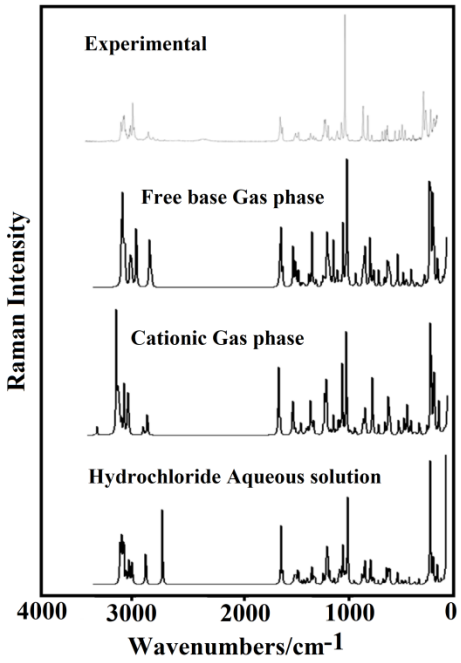

Figure 8. Experimental Raman spectrum of hydrocloride cyclizine species[31] compared with the corresponding predicted for the free base, cationic and hydrochloride species by using B3LYP/6-31G* level of theory.

In particular, when the predicted Raman spectra in activities are converted to intensities by using known equations, as suggested in the literature [50,51]. Here, the intense IR bands observed from 1600 to 400 cm^{-1} can be easily associated to the cationic species because in the IR spectrum predicted for the free base these bands are observed with lower intensities. Here, the SQMFF approach, normal internal coordinates for the three cyclizine species and typical scale factors were used together with the Molvib program in order to obtain the harmonic force fields [26-28]. Then, the vibrational assignments of the spectra were performed considering PED contributions ≥ 10 % and in some cases ≥7% due to strong coupling among some vibration modes. Observed and calculated wavenumbers for the free base, cationic and hydrochloride species of cyclizine in gas phase and in aqueous solution are detailed in **Table 10** together with their corresponding assignments. Some assignments are discussed briefly below.

3.6.1. Band Assignments

3.6.1.1. NH modes. In the experimental IR spectra of hydrochloride cyclizine, the strong and broad band at 2316 cm^{-1}, and at 2312 cm^{-1} in the ATR spectrum is clearly associated to N17-H43 stretching modes because it was predicted by SQM calculations at 2697 cm^{-1}due to that

this group is linked to H43---Cl44 halogen bonds (cyclizine monocation and chloride anion), as was experimentally observed by Bertolasi *et al.* [11]. In hydrochloride species of scopolamine, heroin, morphine, cocaine and tropane alkaloids these N-H stretching modes were predicted by SQM/B3LYP/6-31G* calculations respectively at 1882, 1746, 1776, 2089 and 1760 cm^{-1} [1-3,5-7], in the antihypertensive tolazoline and clonidine agents at 2478 and 1711 cm^{-1} [1-3,5-7] while in the antihistaminic diphenhydramine agent that mode was predicted at 1748 cm^{-1} [8]. In the cationic species of cyclizine this vibration modes is predicted by SQM calculations at 3263 cm^{-1} while in species of scopolamine, heroin, morphine, cocaine and tropane alkaloids these N-H stretching modes were predicted by SQM calculations respectively at 3300, 3268, 3270, 2989 and 3280 cm^{-1} [1-3,5-7], in the antihypertensive tolazoline and clonidine agents at 3312 and 2584 cm^{-1} [1-3,5-7] while in the antihistaminic diphenhydramine agent that mode was predicted at 3150 cm^{-1} [8]. Hence, the weak Raman band at 3087 cm^{-1} can be assigned to that mode for the cationic cyclizine species while the strong ATR band in the hydrochloride spectrum at 2312 cm^{-1} is assigned to the N-H stretching modes. The N atoms of both cationic and hydrochloride species of cyclizine, as in alkaloids, have sp^3 hybridizations for which the normal internal coordinates corresponding to N-H groups are different from those species containing the N atom with sp^2 hybridization [35,37,54-57] because in this latter case the group N-H is planar. Hence, only the rocking modes are expected for both species between 1483 and 1402 cm^{-1} while the in-plane deformation modes are not observed in these two species.

Table 10. Observed and calculated wavenumbers (cm^{-1}) and assignments for the three species of cyclizine in gas and in aqueous solution phases.

Experimental			B3LYP/6-31G* Method[a]							
			Free base				Cationic		Hydrochloride	
			GAS		PCM		GAS		PCM	
IR[c]	ATR[d]	Raman[e]	SQM[b]	Assignments[a]	SQM[b]	Assignments[a]	SQM[b]	Assignments[a]	SQM[b]	Assignments[a]
		3087w	3083	νC5-H24	3090	νC5-H24	3263	νN17-H43	3095	νC13-H30
			3079	νC13-H30	3085	νC13-H30 νC5-H24	3086	νC1-H21	3090	νC5-H24
			3073	νC11-H28	3081	νC1-H21 νC11-H28	3086	νC11-H28	3082	νC11-H28
					3078	νC13-H30	3077	νC13-H30	3081	νC1-H21
					3070	νC2-H22	3075	νC2-H22	3071	νC10-H27
			3072	νC1-H21	3069	νC10-H27	3071	νC10-H27	3070	νC2-H22
					3062	νC12-H29	3068	νC11-H28 νC1-H21	3064	ν_aCH_3
		3062w	3061	νC10-H27	3061	νC6-H25	3065	ν_aCH_3	3064	ν_aCH_3
					3055	νC9-H26	3061	νC12-H29 νC6-H25	3063	νC12-H29
3054w	3053w	3056mw	3060	νC2-H22	3055	νC3-H23	3061	ν_aCH_3	3062	νC6-H25
			3051	νC6-H25			3057	νC5-H24	3056	νC3-H23
3049w			3050	νC12-H29			3050	νC3-H23	3056	νC9-H26
		3044w	3043	νC3-H23			3048	νC9-H26	3037	ν_aCH_2(C18)
			3042	νC9-H26			3036	ν_aCH_2(C16)	3036	ν_aCH_2(C16)
	3026w	3033w					3035	ν_aCH_2(C18)	3010	ν_aCH_2(C15)
	3013w	3012w					3010	ν_aCH_2(C15)	3010	ν_aCH_2(C19)
	3002w	3005w	2998	ν_aCH_2(C19)	3002	ν_aCH_3	3010	ν_aCH_2(C19)	2984	ν_sCH_2(C16)
2975w	2981w	2996w	2998	ν_aCH_2(C15)	2993	ν_aCH_2(C19)	2978	ν_sCH_2(C18)	2979	ν_sCH_2(C18)
		2977s	2987	ν_aCH_3	2992	ν_aCH_2(C15)	2975	ν_sCH_2(C16)	2973	ν_sCH_3
2954sh	2968w	2964w	2947	ν_aCH_2(C18)	2963	ν_aCH_2(C16)	2969	ν_sCH_3		
	2945m	2956w	2942	ν_aCH_2(C16)	2961	ν_aCH_2(C18)				
	2913w		2942	ν_aCH_3	2960	ν_aCH_3	2835	νC7-H31	2857	ν_sCH_2(C15)
2830m	2887w	2847w	2827	ν_sCH_2(C15)	2840	ν_sCH_3			2854	ν_sCH_2(C19)
		2830w	2819	ν_sCH_2(C19)	2835	ν_sCH_2(C15)			2845	νC7-H31
			2815	ν_sCH_3	2834	νC7-H31				
2805w	2807m		2801	ν_sCH_2(C16)	2832	ν_sCH_2(C19)	2801	ν_sCH_2(C15)		
		2819sh			2824	ν_sCH_2(C18)				
		2787w	2796	ν_sCH_2(C18)	2819	ν_sCH_2(C16)				
2549w	2766w	2744w	2792	νC7-H31			2793	ν_sCH_2(C19)		
	2530w	2680vw								
2316vs	2312vs								2697	νN17-H43
	2288vs									
1608w	1607w	1605s	1610	νC12-C13	1604	νC12-C13	1608	νC2-C3	1605	νC12-C13
1608w	1607w	1605s	1605	νC5-C6 νC2-C3	1600	νC5-C6 νC2-C3 νC9-C10	1604	νC5-C6 νC12-C13	1600	νC5-C6 νC2-C3
		1585m	1592	νC10-C11	1587	νC1-C2	1592	νC1-C2 νC8-C13	1587	νC1-C2
1542w	1534w		1589	νC1-C2 νC8-C9	1585	νC10-C11	1589	νC10-C11 νC4-C5	1586	νC3-C4
1503m	1503m	1498w	1498	βC12-H29	1495	βC6-H25	1498	βC12-H29	1497	βC6-H25
	1483m		1494	βC6-H25 βC10-H27	1492	βC9-H26	1495	βC6-H25 βC9-H26	1495	βC12-H29
1480m			1477	δCH_2(C16)	1477	δCH_2(C18) δCH_2(C16)			1483	ρ'N17-H43
			1472	δ_aCH_3	1467	δCH_2(C15)	1468	δCH_2(C15) δCH_2(C19)	1468	ρN17-H43

		1462w	1470	δCH_2(C15)	1464	δCH_2(C16) δCH_2(C18)	1463	$\delta_a CH_3$		
1455s	1456s		1457	βC11-H28	1459	$\delta_a CH_3$	1461	$\delta_a CH_3$	1461	δCH_2(C15)
			1457	βC1-H21	1457	δCH_2(C19)	1460	βC1-H21 βC11-H28	1455	βC1-H21 βC11-H28
			1450	δCH_2(C19)	1455	βC11-H28 βC1-H21	1460	δCH_2(C18) δCH_2(C16)	1452	δCH_2(C18)
1448sh	1449sh	1446sh	1449	$\delta_a CH_3$	1454	βC1-H21 βC11-H28	1454	δCH_2(C15) δCH_2(C19)	1447	δCH_2(C16)
		1433w	1445	δCH_2(C18)	1441	$\delta_a CH_3$	1446	δCH_2(C19) δCH_2(C15)	1439	$\delta_a CH_3$
	1420w	1428w	1425	$wagCH_2$(C16)	1431	$\delta_a CH_3$ $wagCH_2$(C15)	1433	δCH_2(C16) δCH_2(C18)	1438	δCH_2(C19)
1418w	1407w	1411w	1418	$wagCH_2$(C15)	1423	$wagCH_2$(C15)	1429	$wagCH_2$(C15)	1436	$\delta_a CH_3$
							1422	$\delta_s CH_3$	1424	$wagCH_2$(C15)
									1424	δCH_2(C16) δCH_2(C18)
1402w	1388w		1398	$\delta_s CH_3$	1403	$\delta_s CH_3$	1403	$\delta_s CH_3$ ρ'N17-H43	1416	$\delta_s CH_3$ $wagCH_2$(C18)
			1392	$wagCH_2$(C19) $wagCH_2$(C15)	1397	$wagCH_2$(C16)	1402	ρN17-H43	1402	$wagCH_2$(C18) $wagCH_2$(C16)
1382w		1372w	1366	$wagCH_2$(C19) $wagCH_2$(C18)	1374	$wagCH_2$(C19) $wagCH_2$(C18)	1383	$wagCH_2$(C19)	1395	$\delta_s CH_3$
1363sh	1361w				1367	ρ'C7-H31	1369	$wagCH_2$(C16)	1373	$wagCH_2$(C19)
1356w	1352sh	1352sh			1365	ρC7-H31	1362	ρC7-H31	1369	ρ'C7-H31
1348w		1340w	1354	ρC7-H31			1360	$wagCH_2$(C18)	1365	ρC7-H31
			1353	ρ'C7-H31			1355	ρ'C7-H31		
	1328w	1323w	1325	βC13-H30 βC5-H24	1325	βC13-H30 βC5-H24 βC9-H26	1326	βC13-H30	1328	βC13-H30 βC5-H24
1318w			1319	ρCH_2(C16)	1316	βC3-H23	1319	βC3-H23	1320	βC5-H24
		1316sh	1317	βC3-H23	1316	ρCH_2(C16) ρCH_2(C18)	1315	ρCH_2(C16) ρCH_2(C18)	1320	ρCH_2(C16)
	1299w		1300	ρCH_2(C15) ρCH_2(C19)	1300	ρCH_2(C15)	1295	νC3-C4 νC8-C9	1297	ρCH_2(C19) ρCH_2(C15)
1288w	1290m	1292w	1292	νC8-C13 νC3-C4 νC4-C5	1292	νC8-C13 νC3-C4νC8-C9	1284	ρCH_2(C15)	1286	νC8-C13
1278w	1280sh	1273w	1275	ρCH_2(C19) ρCH_2(C15)	1277	ρCH_2(C19)	1282	ρCH_2(C19)	1285	ρCH_2(C19) ρCH_2(C15)
1272w	1263sh	1266sh	1269	ρC7-H31	1264	νC4-C5	1253	ρCH_2(C19)	1256	νC4-C5
1218vw		1220sh	1222	ρCH_2(C18)	1223	ρCH_2(C18) ρCH_2(C16)			1213	ρCH_2(C18)
1209vw	1197m	1209w	1203	ρCH_2(C15) ρCH_2(C19)	1204	ρCH_2(C15)	1200	ρ'CH_3 νN14-C19		
1185m	1189m	1192s	1180	βC2-H22	1181	νC7-C8 νC4-C7	1183	βC2-H22 βC10-H27	1182	νC7-C8νC4-C7 νC8-C9
1179sh		1183s	1178	νC7-C8 νC4-C7	1177	βC3-H23	1182	νC7-C 8νC4-C7	1180	βC3-H23 βC9-H26
1173sh	1174w	1176sh	1173	βC3-H23 βC9-H26	1172	νC4-C7νC7-C8	1176	βC3-H23 βC9-H26	1175	βC6-H25 βC12-H29
1173sh	1174w	1176sh	1172	νC4-C7 νC7-C8	1170	βC10-H27 βC2-H22	1170	νC7-C νC4-C7	1173	ρ'CH_3
1161w			1160	νN17-C20	1158	ρCH_3	1164	βC1-H21	1172	νC4-C7 νC7-C8
1152vw	1154m	1157m	1159	νN17-C20 βC11-H28	1151	βC11-H28	1163	βC11-H28 βC12-H29 βC6-H25	1155	ρCH_3
1152vw	1154m	1157m	1158	βC1-H21 βC11-H28	1150	βC1-H21 βC6-H25 βC12-H29	1160	ρCH_2(C16) ρCH_2(C18)	1151	βC11-H28 βC10-H27 βC2-H22
							1152	ρCH_3	1150	βC1-H21
1142m	1140m		1136	ρCH_3	1136	νN17-C20	1130	ρ'CH_3 νN14-C19 νN14-C15		
1127m	1125w	1124w	1127	νN14-C15	1122	νN14-C19 νN14-C15			1123	νN14-C15 νN14-C19

1111w		1108w	1112	νN14-C7	1100	νN14-C7	1102	νN14-C7	1105	νN14-C7
1085m	1099m	1081sh	1077	νC2-C3	1072	νN14-C7	1075	νN14-C7	1076	βR_1(A3) νN17-C20
1076sh	1071w	1072m	1070	νC9-C10	1069	νC15-C16 νC18-C19	1073	νC9-C10	1074	νC9-C10
1057w	1050sh	1065sh	1061	ρ'CH_3 νC18-C19	1067	ρ'CH_3				
1036sh	1044m	1053w	1037	τR_1(A3) τwCH_2(C19)	1045	τwCH_2(C15)	1035	νN17-C20	1049	νN17-C20
1030m	1033sh	1035m	1026	νC11-C12	1024	νC6-C1	1025	βR_1(A1) βR_1(A2)	1035	νC18-C19 νC15-C16
1017w		1025sh	1025	νC6-C1	1022	βR_1(A2) νC11-C12	1024	νC11-C12 νC6-C1	1028	ρ$CH_3\tau R_1$(A3)
1002w	1002s	1002vs	1002	βR_1(A2)	1004	τwCH_2(C15) τwCH_2(C19)	1012	γC11-H28	1023	βR_1(A1) βR_1(A2)
1002w	1002s	1002vs	1002	βR_1(A1)	1004	νN14-C7	1011	γC1-H21 γC2-H22	1023	νC11-C12 νC6-C1 νC10-C11
1002w	1002s	1002vs					1011	ρ$CH_3\tau R_1$(A3)	1005	γC6-H25
1002w	1002s	1002vs	997	βR_1(A1) βR_1(A2)	997	γC12-H29	1007	νC15-C16 νC18-C19	999	βR_1(A1)
1002w	1002s	1002vs			996	βR_1(A1)	1000	βR_1(A1)	998	βR_1(A2)
	991sh	990sh	993	νC15-C16	995	γC1-H21 γC11-H28	998	βR_1(A2)	998	γC11-H28
986s	991sh	990sh	987	γC6-H25 γC12-H29	993	βR_1(A2)	978	γC12-H29 γC10-H27	991	νN14-C7 νN17-C20
982sh	991sh	990sh	985	γC11-H28 γC1-H21	976	γC10-H27 γC2-H22	972	γC6-H25	981	γC2-H22 γC10-H27
		977w	977	βR_1(A3)	975	βR_1(A3) νN14-C7	970	νN17-C20 νN14-C7	971	γC13-H30
951vw	959w		964	γC2-H22	968	γC6-H25	942	γC9-H26 γC3-H23	965	τwCH_2(C15) τwCH_2(C19) νN17-C16
942m	955sh		956	γC10-H27			940	τwCH_2(C15) τwCH_2(C19)	945	γC3-H23
935sh	938w	935w	929	γC3-H23	934	γC3-H23	928	γC9-H26 γC5-H24	935	γC3-H23
920w			921	τwCH_2(C16)	926	γC9-H26	925	νN17-C20	926	γC5-H24
913sh			910	γC9-H26	913	γC9-H26				
	874m						887	νN17-C18 νN17-C16	898	τwCH_2(C18)
854w	859w	859w	855	γC6-H25 γC12-H29	859	γC9-H26	863	γC3-H23	863	γC12-H29 γC9-H26
		849w	847	γC5-H24 γC13-H30	852	γC5-H24 γC13-H30	853	γC13-H30	856	γC3-H23
			842	νC7-C8 νC4-C7	847	νC7-C8	845	νC7-C8	845	νC7-C8 νC4-C7
837w		832s	836	δC4C7C8	837	δC4C7C8	836	δC4C7C8	838	νN14-C19 νN14-C15
826vw			833	δC4C7N14 δC8C7N14 νN14-C19	834	δC4C7N14	824	δC4C7N14 δC8C7N14	832	δC4C7N14 δC8C7N14
805vw	815w	790s	800	τwCH_2(C15) τwCH_2(C19) τwCH_2(C18)	807	τwCH_2(C19) τwCH_2(C15) τwCH_2(C18) τwCH_2(C16)	766	τwCH_2(C18) τwCH_2(C16)	778	τwCH_2(C16)
792w	777s		767	νN17-C18 νN17-C16	772	νN17-C18 νN17-C16	761	τR_1(A2)	768	νN17-C18
755s		752w	755	τR_1(A2) τR_1(A1)	757	τR_1(A2) τR_1(A1)	757	τR_1(A1) τR_1(A2)	753	γC1-H21
	738vs		749	τR_1(A1) τR_1(A2)	751	τR_1(A1) τR_1(A2)	743	νN17-C18 νN17-C16	753	τR_1(A2)
715vs	727s	707vw	706	τR_1(A2)	706	τR_1(A2) τR_1(A1)	708	τR_1(A1) τR_1(A2)	710	τR_1(A2)
700m	681w		690	τR_1(A1)	692	τR_1(A1)	692	τR_1(A2)	695	τR_1(A1)
700m	681w				670	βR_1(A3)				
656w	658m	655m	654	βR_3(A1)	644	βR_3(A2) βR_3(A1)	651	τR_1(A1)	660	βR_1(A3)

639w		634	βR_3(A2)			631	βR_2(A2)	638	βR_3(A2)
636w		632	βR_3(A1)	631	βR_3(A2) βR_3(A1)	631	βR_3(A2) βR_3(A1)	631	βR_3(A1)
628w	629m	621	βR_2(A1)	627	βR_2(A1) βR_2(A2)			626	βR_2(A1)
	613sh	618	βR_2(A2)	618	βR_2(A1) βR_2(A2)	618	βR_2(A1)	618	βR_2(A2)
	607m					608	βR_1(A3)		
568m	569w			551	τR_1(A2)				
528m	536m	544	τR_1(A1) τR_1(A2)	531	βR_2(A3)	532	τR_1(A1) τR_1(A2)	542	τR_1(A2) τR_1(A1)
502m	496m	500	βR_2(A3)			491	βR_2(A3)	505	βR_2(A3)
473m	469s	473	τR_2(A2)	477	τR_2(A1) τR_2(A2)	471	τR_2(A2) γC4-C7	477	τR_2(A2) τR_2(A1)
473m	469s	464	τR_1(A3) τR_2(A1)	476	τR_1(A3) γN14-C7	461	τR_1(A3)	468	τR_1(A3) δC16N17C20
437w	441m	422	τR_1(A3) βR_3(A3)	437	τR_1(A3) βR_3(A3)	436	βR_3(A3)	446	βR_3(A3)
	407w	408	τR_3(A1)	409	τR_3(A2)				
	407w	402	τR_3(A2)	403	τR_3(A1)	406	τR_3(A1)	414	τR_3(A1)
				394	τR_2(A3) γN14-C7	399	τR_3(A2)	406	τR_3(A2)
	369w	379	βN17-C20	380	βN17-C20	397	γN14-C7	398	γN14-C7
	364sh	354	γN17-C20	346	τR_3(A3)	365	δC16N17C20	367	δC16N17C20 δC18N17C20
	307w	313	τR_3(A3) βN17-C20						
				293	γN17-C20 γN14-C7	303	δC18N17C20	304	τR_3(A3)
	285sh			292	βC8-C7 βC4-C7	270	τR_3(A3) βC4-C7 βC8-C7	286	τR_1(A3)
	271vs	274	τR_3(A3) βC4-C7 βC8-C7	263	τR_2(A1)	267	τR_2(A1)	277	τR_3(A3) βC4-C7 βC8-C7
	251s	266	τR_2(A1)	259	τwCH$_3$			267	τR_2(A1) τR_2(A2)
		246	βR_3(A3) νN14-C7	243	βN14-C7	243	νN14-C7 βR_3(A3)	243	τR_3(A3) βC4-C7
	239sh	236	τwCH$_3$ τR_3(A3)	239	νN14-C7 γN14-C7	237	τR_1(A3) γN14-C7	239	γN14-C7 βR_3(A3)
	230sh	236	γN14-C7			230	τR_3(A3)		
	219sh	222	τwCH$_3$			204	τwCH$_3$	219	τwCH$_3$
	204s	196	τR_2(A2) τR_2(A1)	200	τR_2(A2)	192	τR_3(A3) τR_2(A2)	199	βN14-C7
	176w							161	νH43-Cl44
	146w	143	τR_2(A3)	149	τR_2(A3)	139	τR_2(A3)		
				87	τR_2(A3) γN14-C7			148	τR_2(A3) δN17H43Cl44
				81	δC8C7N14			92	δN17H43Cl44
		76	τ_wN14-C7 γC8-C7			75	τ_wN14-C7 γC8-C7	76	τC4-C7
		74	τC4-C7 τC8-C7	66	τC4-C7	74	τC4-C7	74	τC4-C7 τN17-H43
				65	τ_wN14-C7 C4-C7			64	τN17-H43
		55	βN14-C7			50	τR_2(A3) γN14-C7	50	δC4C7C8 γC4-C7 γC8-C7
		52	γC4-C7	43	γC8-C7	49	βN14-C7	41	τC8-C7
						46	δC4C7C8	37	τR_2(A3)
		13	τC8-C7 τC4-C7	22	τC8-C7	13	τC8-C7	23	τ_wN14-C7

Abbreviations: ν, stretching; β, deformation in the plane; γ, deformation out of plane; wag. wagging; τ , torsion; β_R. deformation ring τ_R. torsion ring; ρ. rocking; τw. twisting; δ. deformation; a. antisymmetric; s. symmetric; (A_1). Ring 1; [a]This work, [b]From scaled quantum mechanics force field, [c]From Ref [29], [d]From Ref [30], [e]From Ref [31].

3.6.1.2. CH modes. The aromatic C-H modes belonging to the two phenyl rings are predicted by SQM calculations in the three species of cyclizine between 3095 and 3042 cm^{-1}while the only aliphatic C-H stretching modes are predicted in different regions in the three species of cyclizine. Thus, in the free base, cationic and hydrochloride species these modes are predicted at 2792, 2834 and 2845 cm^{-1}, respectively and, for these reasons, they were assigned accordingly, as mentioned in Table 10.The aromatic C-H in-plane and out-of-plane deformation modes are assigned to the IR and Raman bands between 1498/1150 and 1012/847 cm^{-1}while the aliphatic C-H rocking modes for the three species are assigned between 1369 and 1353cm^{-1}, as detailed in Table 10.

3.6.1.3. CH_3 modes. In the three cyclizine species there is only one CH_3 group for which nine vibration normal modes are expected for each species. The two expected antisymmetric stretching modes are predicted in the free base, cationic and hydrochloride species at 2987/2942, 3002/2960 and 3064 cm^{-1} while the corresponding symmetric ones at 2815, 2840 and 2973 cm^{-1}, respectively. In cocaine species, these modes were assigned between 3056 and 2845 cm^{-1} [3] while in tropane species between 3098 and 2966 cm^{-1}[2]. Note that in the free base species these modes are predicted at lower wavenumbers than the other ones and that the strong Raman band at 2977cm^{-1} is clearly assigned to symmetric modes. The antisymmetric and symmetric deformation modes in tropane and cocaine species [2,3] are predicted between 1478/1400 and 1474/1409 $cm^{-1}$and, for this reason, these modes in the three cyclizine species are clearly assigned between 1472 and 1398 cm^{-1}, as observed in Table 10.In the cocaine and tropane species the rocking modes were predicted respectively between 1194/1134 and 1183/1128 cm^{-1} while the twisting modes were assigned between 191/117 and 205/151 cm^{-1}[2,3]. Hence, in the three cyclizine species rocking and twisting modes were assigned between 1200/1011 and 259/204 cm^{-1}, as predicted by SQM calculations.

3.6.1.4. CH_2 modes. Each cyclizine species has four CH_2 groups that belong to the piperazine ring, for which, a total of twenty four vibration modes are expected for each species. The antisymmetric and symmetric stretching modes in cocaine and tropanespecies

were assigned between 3009/2938 and 3024/2911 cm^{-1}[2,3] while these modes in the three cyclizine species were predicted by SQM calculations between 3037 and 2793 cm^{-1}, as can be seen in Table 10. Hence, the IR and Raman bands observed in that region are associated to those vibration modes. The deformation, wagging, rocking and twisting modes expected for these groups were predicted in cocaine species at 1483/1449, 1382/1242, 1230/1167 and 933/744 cm^{-1} while in the tropane species, these modes were assigned respectively at 1485/1442, 1385/1274, 1274/1142 and 967/639 cm^{-1}. In similar compounds these modes were assigned in approximately the same regions [34-39,41,42,54,55-57]. Hence, in the three cyclizine species the deformation, wagging, rocking and twisting modes are attributed to the IR and Raman bands observed at 1477/1438, 1433/1360, 1319/1203 and 1037/766, respectively as indicated in Table 10.

3.6.1.5. Skeletal modes. The N-CH_3 stretching modes in the cyclicine species (N17-C20) are predicted in different regions, thus, in the free base in gas phase that mode is predicted at 1160 cm^{-1} while in solution is observed at 1136 cm^{-1} due to the hydration, in the cationic and hydrochloride species are predicted at 1035 and 1049 cm^{-1}, respectively. In the free base, cationic and hydrochloride species of cocaine those stretching modes were predicted respectively at 1113, 1058 and 1052 cm^{-1} while in the tropane species these modes are predicted at 1128, 1086 and 1031 cm^{-1}[2,3]. Hence, in the cyclizine species these modes are quickly associated to the IR and Raman bands observed in those regions. The IR and Raman bands observed with different intensities between 1608 and 1534 cm^{-1} are clearly associated to the C=C stretching modes of two phenyl rings while the other C-N stretching modes related to the piperazine rings (N14-C7, N14-C15, N14-C19, N17-C16, N17-C18) are predicted in the three species in different regions, as observed in Table 10. Thus, the strong Raman bands at 1605, 1192, 1002, 832 and 790 cm-1 are associated to C-C and C-N stretching modes of those three species of cyclizine. In the same way, the strong ATR bands at 1002, 777 and 738 cm^{-1} are also related to those vibration modes of three cyclizine species.On the other hand, three deformations and three torsions rings are expected for each phenyl ring (A1 and A2) and for the piperazine rings (A3).These vibration modes were predicted strongly coupled in the three species of cyclizine and, for these reasons, some IR, ATR and Raman bands observed with different intensities from 752 up to 146 cm^{-1} were assigned to more than one vibration mode. All these vibration modes together with the remain modes [1-3,5-8,34-42,52-57] were assigned taking into account the SQM calculations and the assignments reported for similar compounds, as was descript in Table 10.

4. Force constants

The harmonic force constants for the free base, cationic and hydrochloride species of cyclizine were computed from the corresponding harmonic force fields by using the SQMFF methodology [26,27] and the Molvib program [28] at the B3LYP/6-31G* level of theory.**Table 11** shows the most important force constants for those three species of cyclizine in different media. Analyzing these values in exhaustive form, we observed that the cationic species presents a *f(νN-H)*force constant higher than the hydrochloride species in solution, as was also observed between these two species of scopolamine, heroin, morphine, cocaine, tropane alkaloids [1-3,5-8].

Table 11. Scaled internal force constants for the free base, cationic and hydrochloride cyclizine species in gas and aqueous solution phases by using the B3LYP/6-31G* method.

Force constant	Cyclizine[a]			
	Free base		Cationic	Hydrochloride
	Gas	PCM	Gas	PCM
$f(\nu N\text{-}H)$			5.91	4.61
$f(\nu N\text{-}CH_3)$	4.85	4.69	4.06	4.33
$f(\nu C\text{-}N)$	4.54	4.45	4.13	4.19
$f(\nu CH_2)$	4.62	4.65	4.82	4.87
$f(\nu CH_3)$	4.69	4.76	5.06	5.07
$f(\nu C\text{-}H)_R$	5.15	5.17	5.17	5.18
$f(\nu C\text{-}H)$	4.31	4.44	4.44	4.74
$f(\nu C\text{-}C)$	6.50	6.46	6.50	6.46
$f(\delta CH_2)$	0.74	0.75	0.73	0.73
$f(\delta CH_3)$	0.58	0.57	0.56	0.55

Units are mdyn $Å^{-1}$ for stretching and mdyn Å rad^{-2} for angle deformations

[a]This work

These results can be justified by the shorter N-H distances predicted in all cases due to their positive charges. On the contrary, the *f(νN-CH₃)*constants present higher values in the free base in both media, as expected because the presences of H atoms forming N-H bonds in the

cationic and hydrochloride species generate a enlargement of N-CH_3 bonds diminishing their corresponding force constants. In the same way, the higher N-CH_3 distances in the cationic and hydrochloride species could also justify their low *f(νC-N)*constants values, as compared with the values observed for the free base species in both media. On the other hand, the slight increase in the *f(νCH₃)*force constants values of the cationic and hydrochloride species could be related to the high negative charges values observed on the C20 atoms belonging to CH_3 groups in those two species, as was previously analyzed in section 3.3. Finally, the *f(νC-H)*force constant of hydrochloride species presents a slight higher value in the hydrochloride species probably due to the presence of strong electronegativity of Cl atom that notably stabilize this species by different delocalization, as supported by NBO studies.

5. Electronic spectrum

The electronic spectra of cyclizine species are of great interest in pharmaceutical chemistry because the hydrochloride species is usually used in the preparation of pharmaceutical formulation and biological fluids, as mentioned by Bohlokoand Al-Shaalan[14,17]. Here, for the free base and hydrochloride species of cyclizine were predicted the ultraviolet-visible spectra in aqueous solution by using the B3LYP/6-31G* method while the B3LYP/6-31+G* method support clearly the existence of cationic species in solution. The experimental spectrum of hydrochloride cyclizine [12] shows two bands, a strong at 229.3 nm and other of lower intensity at 230 nm while the predicted spectra of free base, cationic hydrochloride species in solution present a strong band at229.3 nm,245.2 nm and 324 nm, respectively. Obviously, the most intense band could be attributed to the$\pi \rightarrow \pi^*$ transitions due to the presence of C=C double bonds of both phenyl rings, as reported for similar species containing C=C bonds [58,59] while the weakest band could be associated to $n \rightarrow n^*$ transitions that are also predicted by NBO calculations for hydrochloride species in solution.

5. CONCLUSIONS

In the present work, the theoretical structures of free base, cationic and hydrochloride species of cyclizine have been determined in gas phase and in aqueous solution by using the hybrid B3LYP/6-31G* method. In solution, the SCRF methodology was employed with the PCM method and the universal solvation model to compute the solvation energies. Stable structures were obtained for free base in both media, for the cationic species in gas phase and for the hydrochloride species in solution, as supported by their positive frequencies. The

existence of cationic form in solution was verified by using the 6-31+G* level of theory. The force fields of those three species in both media were computed in order to perform the complete vibrational assignments of experimental available IR, ATR and Raman spectra by using the normal internal coordinates, the SQMFF methodology and the Molvib program. Here, the complete assignments of expected 120, 123 and 126 vibration modes for free base, cationic and hydrochloride species of cyclizine and their corresponding force constants are reported for first time. The predicted infrared, Raman and ultraviolet-visible spectra have evidenced reasonable correlations with the corresponding experimental ones.

The free base of cyclizine presents the lower solvation energy value, as compared with scopolamine, heroin, morphine, cocaine and tropane alkaloids. The calculations have predicted for the three cyclizine species similarities in some geometrical parameters showing clearly that both phenyl rings are symmetric, as was experimentally observed. The studies of N-CH_3 distances in the three species have evidenced that the free base of cyclizine in solution presents practically the same value than heroin and morphine in the same medium. This similarity in the values could be attributed to that N-CH_3 group in cyclizine is linked only to a ring(piperazine), as in heroin and morphine and not to bicyclic rings as in cocaine, scopolamine and tropane alkaloids. Evidently, the N-C distances are shortened when the N-CH_3 group is linked to two fused rings.

The mapped MEP surfaces reveal different nucleophilic and/or electrophilic regions in the three species of cyclizine where probable reactions can take place.

NBO studies show clearly that the high stabilities of free base and hydrochloride species are strongly related to the presence of $\pi \rightarrow \pi^*$ transitions due to the two phenyl rings in their structures while AIM analyses clearly supports the high stability of hydrochloride species in solution due to the two interactions, H24---H30 and ionic H43---Cl44 interaction, where the strong ionic interaction is clearly evidenced by their highest topological properties.

ACKNOWLEDGEMENTS

This work was supported with grants from CIUNT Project Nº 26/D608(Consejo de Investigaciones, Universidad Nacional de Tucumán). The authors would like to thank Prof. Tom Sundius for his permission to use MOLVIB.

REFERENCES

[1] Brandán SA, Why morphine is a molecule chemically powerful. Their comparison with cocaine, Indian Journal of Applied Research, 2017; 7(7): 511-528.
[2] Rudyk RA, Brandán SA, Force field, internal coordinates and vibrational study of alkaloid tropane hydrochloride by using their infrared spectrum and DFT calculations, Paripex A Indian Journal of Research, 2017; 6(8): 616-623.
[3] Romani D, Brandán SA, Vibrational analyses of alkaloid cocaine as free base, cationic and hydrochloride species based on their internal coordinates and force fields, Paripex A Indian Journal of Research, 2017; 6(9): 587-602.
[4] Iramain MA, Ledesma AE, Brandán SA, Analyzing the effects of halogen on properties of a halogenated series of R and S enantiomers analogues alkaloid cocaine-X, X=F, Cl, Br, I., Paripex A Indian Journal of Research, 2017; 6(12): 454-463.
[5] Brandán SA, Understanding the potency of heroin against to morphine and cocaine, IJSRM, International Journal of Science And Research Methodology,2018; 12(2): 97-140.
[6] Rudyk RA, Checa MA, Catalán CAN, Brandán SA, Structural, FT-IR, FT-Raman and ECD spectroscopic studies of free base, cationic and hydrobromide species of scopolamine alkaloid, submitted to J. Mol. Struct. 2018; 1180: 603-617.
[7] Rudyk RA, Checa MA, Guzzetti KA, Iramain MA, Brandán SA, Behaviour of N-CH_3 Group in Tropane Alkaloids and correlations in their Properties, IJSRM, International Journal of Science And Research Methodology, 2018; 10 (4): 70-97.
[8] Iramain MA, Brandán SA, Structural and vibrational properties of three species of anti-histaminic diphenhydramine by using DFT calculations and the SQM approach, Journal: To Chemistry Journal,2018; 1(1):105-130.
[9] Russell JT, Cyclizine anaphylaxis, when administered with propanidid, Anaesthesia. 1969; 24(1):76-80
[10] Klawans HL, Moskovitz C., Cyclizine-induced chorea. Observations on the influence of cyclizine on dopamine-related movement disorders, J Neurol Sci. 1977; 31(2):237-44.
[11] V. Bertolasi, P. A. Borea, G. Gilli AND M. Sacerdoti, Cyclizine Hydrochloride, Acta Cryst. 1980; B36: 1975-1977.
[12] Walker RB, HPLC analysis and pharmacokinetics of cyclizine, Doctoral Thesis, School of Pharmaceutical Sciences, Rhodes University, Grahamstown, 1995.
[13] Laffey JG, Boylan JF., Cyclizine and droperidol have comparable efficacy and side effects during patient-controlled analgesia, Ir J Med Sci. 2002; 171(3):141-144.
[14] Bohloko N.S., Development and formulation of an intranasal dosage form for cyclizine hydrochloride, Doctoral Thesis, Faculty of Health Sciences at the Department of Pharmaceutics, Potchefstroom University for Christian Higher Education, Potchefstroom, 2003.
[15] O'Brien CM, Titley G, Whitehurst P., A comparison of cyclizine, ondansetron and placebo as prophylaxis against postoperative nausea and vomiting in children, Anaesthesia. 2003; 58(7):707-711.
[16]H King, P Corry, T Wauchob, P Barclay, Probable dystonic reaction after a single dose of cyclizine in a patient with a history of encephalitis, Anaesthesia,2003; 58(3): 257-60.
[17] Al-Shaalan NH, Extractive spectrophotometric assay of cyclizine in a pharmaceutical formulation and biological fluids, Saudi Pharmaceutical Journal,2012; 20: 255–262.
[18] Cao D-S, Zhang L-X, Tan G-S, Xiang Z., Zeng W-B, Xu Q-S, Che AF, Computational Prediction of Drug-Target Interactions Using Chemical, Biological, and Network Features, Molecular informatics, 2014; 33(10): 669-681.
[19] Abhyankar D, Shedage A, Gole M, Raut P, Bioequivalence study of cyclizine hydrochloride 50 mg tablets in healthy volunteers: a randomized, open-label, single-dose study, Therapeutic Delivery,2016; 7(8):545-551.
[20] He S, Xiao J, Dulcey AE, Lin B, Rolt A, Hu Z, Hu X, Wang AQ, Xu X, Southall N, Ferrer M, Zheng W, Liang TJ, Marugan JJ., Discovery, Optimization, and Characterization of Novel Chlorcyclizine Derivatives for the Treatment of Hepatitis C Virus Infection, J. Med. Chem.,2016; 59(3): 841–853.
[21] Becke AD, Density-functional exchange-energy approximation with correct asymptotic behavior, Phys. Rev. 1988; A38: 3098-3100.

[22] Lee C, Yang W, Parr RG. Development of the Colle-Salvetti correlation-energy formula into a functional of the electron density, Phys. Rev. 1988; B37: 785-789.
[23] Miertus S, Scrocco E, Tomasi J. Electrostatic interaction of a solute with a continuum. Chem. Phys. 1981; 55:117–129.
[24] Tomasi J, Persico J. Molecular Interactions in Solution: An Overview of Methods Based on Continous Distributions of the Solvent. Chem. Rev. 1994; 94:2027-2094.
[25] Marenich AV, Cramer CJ, Truhlar D.G. Universal solvation model based on solute electron density and a continuum model of the solvent defined by the bulk dielectric constant and atomic surface tensions. J. Phys. Chem. 2009; B113:6378-6396.
[26] Pulay, P.; Fogarasi, G.; Pongor, G.; Boggs, J. E.; Vargha, A. Combination of theoretical ab initio and experimental information to obtain reliable harmonic force constants. Scaled quantum mechanical (QM) force fields for glyoxal, acrolein, butadiene, formaldehyde, and ethylene, J. Am. Chem. Soc. 1983; 105: 7073.
[27] Rauhut G, Pulay P, Transferable Scaling Factors for Density Functional Derived Vibrational Force Fields, J.Phys. Chem. 1995; 99: 3093-3100. b) Correction: G. Rauhut, P. Pulay, J. Phys. Chem. 1995; 99: 14572.
[28] Sundius T. Scaling of ab-initio force fields by MOLVIB. Vib. Spectrosc. 2002; 29:89-95.
[29] Infrared spectrum available from: https://webbook.nist.gov/cgi/inchi?
[30] ATR spectrum available from: https://spectrabase.com/spectrum/JBbr0wHcL96
[31] Raman spectrum available from:https://spectrabase.com/spectrum/1fQR8QLIvZT
[32] Parr RG, Pearson RG, Absolute hardness: companion parameter to absolute electronegativity, J. Am. Chem. Soc. 1983; 105: 7512-7516.
[33] Brédas J-L, Mind the gap!, Materials Horizons,2014; 1: 17–19.
[34] Romani D, Brandán SA, Márquez MJ, Márquez MB, Structural, topological and vibrational properties of an isothiazole derivatives series with antiviral activities, J. Mol. Struct. 2015; 1100: 279-289.
[35] Romani D, Tsuchiya S, Yotsu-Yamashita M, Brandán SA, Spectroscopic and structural investigation on intermediates species structurally associated to the tricyclic bisguanidine compound and to the toxic agent, saxitoxin, J. Mol. Struct. 2016; 1119: 25-38.
[36] Romano E, Castillo MV, Pergomet JL, Zinczuk J, Brandán SA, Synthesis, structural and vibrational analysis of (5,7-Dichloro-quinolin-8-yloxy) acetic acid, J. Mol. Struct. 2012; 1018: 149–155.
[37] Chain FE, Ladetto MF, Grau A, Catalán CAN, Brandán SA, Structural, electronic, topological and vibrational properties of a series of N-benzylamides derived from Maca (Lepidium meyenii) combining spectroscopic studies with ONION calculations, J. Mol. Struct. 2016; 1105: 403-414.
[38] Chain F, Iramain MA, Grau A, Catalán CAN, Brandán SA, Evaluation of the structural, electronic, topological and vibrational properties of N-(3,4-dimethoxybenzyl)-hexadecanamide isolated from Maca (Lepidium meyenii) using different spectroscopic techniques, J. Mol. Struct. 2016; 1119: 25-38.
[39] Minteguiaga M, Dellacassa E., Iramain MA, Catalán CAN., Brandán SA, A structural and spectroscopic study on carquejol, a relevant constituent of the medicinal plant Baccharis trimera (Less.) DC. (Asteraceae), J. Mol. Struct. 2017; 1150: 8-20.
[40] Iramain MA, Davies L, Brandán SA, Structural and spectroscopic differences among the Potassium 5-hydroxypentanoyltrifluoroborate salt and the furoyl and isonicotinoyl salts, J Mol. Struct. 2019; 1176: 718-728.
[41] Issaoui N, Ghalla H, Brandán SA, Bardak F, Flakus HT, Atac A, Oujia B, Experimental FTIR and FTRaman and theoretical studies on the molecular structures of monomer and dimer of 3-thiopheneacrylic acid, J. Mol. Struct. 2017; 1135: 209-221.
[42]Minteguiaga M, Dellacassa E, Iramain MA, Catalán CAN, Brandán SA, FT-IR, FT-Raman, UV-Vis, NMR and structural studies of Carquejyl Acetate, a component of the essential oil from *Baccharis trimera* (Less.) DC. (Asteraceae), submitted to J Mol. Struct. 2019; 1177: 499-510.
[43] Nielsen AB, Holder AJ, Gauss View 3.0, User's Reference, GAUSSIAN Inc., Pittsburgh, PA, 2000–2003.
[44] Gaussian 09, Revision A.02, Frisch, M. J.; Trucks, G. W.; Schlegel, H. B.; Scuseria, G. E.; Robb, M. A.; Cheeseman, J. R.; Scalmani, G.; Barone, V.; Mennucci, B.; Petersson, G. A.; Nakatsuji, H.; Caricato, M.; Li, X.; Hratchian, H. P.; Izmaylov, A. F.; Bloino, J.; Zheng, G.; Sonnenberg, J. L.; Hada, M.; Ehara, M.; Toyota, K.; Fukuda, R.; Hasegawa, J.; Ishida, M.; Nakajima, T.; Honda, Y.; Kitao, O.; Nakai, H.; Vreven, T.; Montgomery, J. A., Jr.; Peralta, J. E.; Ogliaro, F.; Bearpark, M.; Heyd, J. J.; Brothers, E.; Kudin, K. N.; Staroverov, V. N.; Kobayashi, R.; Normand, J.; Raghavachari, K.; Rendell, A.; Burant, J. C.; Iyengar, S. S.;

Tomasi, J.; Cossi, M.; Rega, N.; Millam, J. M.; Klene, M.; Knox, J. E.; Cross, J. B.; Bakken, V.; Adamo, C.; Jaramillo, J.; Gomperts, R.; Stratmann, R. E.; Yazyev, O.; Austin, A. J.; Cammi, R.; Pomelli, C.; Ochterski, J. W.; Martin, R. L.; Morokuma, K.; Zakrzewski, V. G.; Voth, G. A.; Salvador, P.; Dannenberg, J. J.; Dapprich, S.; Daniels, A. D.; Farkas, Ö.; Foresman, J. B.; Ortiz, J. V.; Cioslowski, J.; Fox, D. J. Gaussian, Inc., Wallingford CT, 2009.

[45] Ugliengo P, Moldraw Program, University of Torino, Dipartimento Chimica IFM, Torino, Italy, 1998.

[46] Besler BH, Merz KM Jr, Kollman PA, Atomic charges derived from demiempirical methods, J. Comp. Chem.1990; 11: 431-439.

[47] Glendening ED, Badenhoop JK, Reed AD, Carpenter J E, Weinhold F, NBO 3.1; Theoretical Chemistry Institute, University of Wisconsin; Madison, WI, 1996.

[48] Biegler-Köning F, Schönbohm J, Bayles D, AIM2000; A Program to Analyze and Visualize Atoms in Molecules, J. Comput. Chem. 2001; 22: 545.

[49] Bader RFW, Atoms in Molecules, A Quantum Theory, Oxford University Press, Oxford, 1990, ISBN: 0198558651.

[50] Keresztury G, Holly S, Besenyei G, Varga J, Wang AY, Durig JR, Vibrational spectra of monothiocarbamates-II. IR and Raman spectra, vibrational assignment, conformational analysis and ab initio calculations of S-methyl-N,N-dimethylthiocarbamate, Spectrochim. Acta, 1993; 49A: 2007-2026.

[51] Michalska D, Wysokinski R, The prediction of Raman spectra of platinum(II) anticancer drugs by density functional theory, Chem. Phys Letters, 2005; 403: 211-217.

[52] C. D. Contreras, A. E. Ledesma, J. Zinczuk, S. A. Brandán, Vibrational study of tolazoline hydrochloride by using FTIR-Raman and DFT calculations, Spectrochim. Acta A, 79 (2011) 1710-1714.

[53] Elida Romano, Alicia B. Brizuela, Karina Guzzetti, S. A. Brandán, An experimental and theoretical study on the Hydration in aqueous medium of the antihypertensive agent tolazoline hydrochloride, J. Molec. Struct. 1037 (2013) 393-401.

[54] Elida Romano, Lilian Davies, Silvia Antonia Brandán, Structural properties and FTIR-Raman spectra of the anti-hypertensive, clonidine hydrochloride agent and their dimeric species, Journal of Molecular Structure 1133 (2017) 226-235.

[55] Márquez MJ, Márquez MB, Cataldo PG, Brandán SA, A Comparative Study on the Structural and Vibrational Properties of Two Potential Antimicrobial and Anticancer Cyanopyridine Derivatives, Open Journal of Synthesis Theory and Applications, 2015; 4: 1-19.

[56] Márquez MB, Brandán SA, A Structural and Vibrational Investigation on the Antiviral Deoxyribonucleoside Thymidine Agent in Gas and Aqueous Solution Phases, Int. J. Quantum Chem. 2014; 114: 209-221.

[57] Cataldo PG, Castillo MV, Brandán SA, Quantum Mechanical Modeling of Fluoromethylated-pyrrol Derivatives a Study on their Reactivities, Structures and Vibrational Properties, J Phys Chem Biophys, 2014; 4(1): 4-9.

[58] Chain FE, Leyton P, Paipa C, Fortuna M, Brandán SA, FT-IR, FT-Raman, UV-Visible, and NMR spectroscopy and vibrational properties of the labdane-type diterpene 13-epi-sclareol, Spectrochim. Acta Part A,2015; 138: 303-313.

[59] Bruno TJ, Svoronos PDN, CRC Handbook of Basic Tables for Chemical Analysis, Second Edition, CRC Press, Taylor & Francis Goup, Boca Raton, 2011.